Thermal analysis of ice and glass transitions in insects that do and do not survive freezing.

Jan Rozsypal, Martin Moos, Petr Šimek, Vladimír Koštál*

Biology Centre of the Czech Academy of Sciences,
Institute of Entomology, 37005 České Budějovice, Czech Republic

* Correspondence: kostal@entu.cas.cz

Summary statement:

Using differential scanning calorimetry, we measured ice fraction dynamics during gradual cooling after inoculative freezing in variously acclimated larvae of two drosophilid flies.

Abbreviations:

DM, dry mass; DSC, differential scanning calorimtery; FM, fresh mass; IF, relative ice fraction; IF_{max}, maximum ice fraction; LN_2, liquid nitrogen; m.p., melting point; OAW, osmotically active body water; OIW, osmotically inactive body water; T, temperature; T_{dg}, temperature of de-glassing transition; T_g, temperature of vitrification; T_{EM}, equilibrium temperature; T_{INO}, temperature of inoculation of body fluids by external ice crystals; T_{SCP}, temperature of spontaneous freezing (supercooling point); TBW, total body water

Key words:

insects, freeze tolerance, ice fraction, osmotically inactive water, proline, vitrification

ABSTRACT

Some insects rely on the strategy of freeze tolerance for winter survival. During freezing, extracellular body water transitions from the liquid to solid phase and cells undergo freeze-induced dehydration. Here we present results of a thermal analysis (from differential scanning calorimetry) of ice fraction dynamics during gradual cooling after inoculative freezing in variously acclimated larvae of two drosophilid flies, *Drosophila melanogaster* and *Chymomyza costata.* Although the species and variants ranged broadly between 0 and close to 100% survival of freezing, there were relatively small differences in ice fraction dynamics. For instance, the maximum ice fraction (IF_{max}) ranged between 67.9 and 77.7% total body water (TBW). The *C. costata* larvae showed statistically significant phenotypic shifts in parameters of ice fraction dynamics (melting point and IF_{max}) upon entry into diapause, cold-acclimation, and feeding on a proline-augmented diet. These differences were mostly driven by colligative effects of accumulated proline (ranging between 6 and 487 $mmol.kg^{-1}$ TBW) and other metabolites. Our data suggest that these colligative effects *per se* do not represent a sufficient mechanistic explanation for high freeze tolerance observed in diapausing, cold-acclimated *C. costata* larvae. Instead, we hypothesize that accumulated proline exerts its protective role via a combination of mechanisms. Specifically, we found a tight association between proline-induced stimulation of glass transition in partially-frozen body liquids (vitrification) and survival of cryopreservation in liquid nitrogen.

INTRODUCTION

Insects overwintering in temperate and polar habitats have evolved different cold tolerance strategies to cope with situations when their body temperature decreases below the equilibrium melting point (Salt, 1961; Lee, 2010). Some insect species show only limited capacity for cold tolerance and are often classified as chill susceptible (Bale, 1993; 1996; Koštál et al., 2011a). The overwintering strategies of truly cold tolerant insects are categorized as freeze avoidance, i.e. reliance on supercooling of body liquids (Zachariassen, 1985; Renault et al., 2002), or freeze tolerance, i.e. survival after formation of ice crystals inside body (Sinclair et al., 2003; Sinclair

and Renault, 2010). Some insects use the strategy of cryoprotective dehydration, i.e. lose most of their body water by evaporation and deposition to surrounding ice crystals in their overwintering microhabitat (Holmstrup and Westh, 1994; Holmstrup et al., 2002). Under specific conditions, insect body solutions may also undergo phase transition into a biological glass via the process of vitrification (Sformo et al., 2010; Koštál et al., 2011b).

In this paper, we focus on the strategy of freeze tolerance. The classical view (Lovelock, 1954; Asahina, 1969) is that freeze-tolerant organisms rely on formation of ice crystal nuclei in extracellular space. As the ice nuclei grow with decreasing temperatures, the extracellular solutions become more concentrated, which osmotically drives water out of cells. It remains debated whether and how often intracellular ice formation occurs *in vivo* and whether or not it is always lethal (Wharton and Ferns, 1995; Sinclair and Renault, 2010). In this particular study on dipteran larvae, we adhere to the classical model of extracellular ice formation that is also supported by our direct observations of extracellular ice masses in frozen larvae of *Chymomyza costata* by scanning electron microscopy of cryo-fractured specimens (Koštál et al., 2011b). Considering the classical model, a freeze-tolerant insect must cope with not only deep sub-zero body temperature but also the multiple deleterious effects linked to freeze-induced cellular dehydration (Muldrew et al., 2004; Sinclair and Renault, 2010). All of these effects threaten the chemical and conformational stability of proteins and other macromolecules (Wang, 1999; Brovchenko and Oleinikova, 2008). In order to alleviate the stresses linked with extracellular freezing, freeze-tolerant insects often synthesize and accumulate a variety of small cryoprotective molecules (Somme, 1982; Storey and Storey, 1991; Koštál et al., 2016a) and/or macromolecular compounds that regulate the process of ice formation (Zachariassen and Kristiansen, 2000; Duman, 2001; 2015). Under eco-physiological conditions, only a certain fraction of the insect's total body water is freezable (*i.e.* osmotically active water, OAW; corresponding to maximum ice fraction), while the rest is unfreezable (*i.e.* osmotically inactive water, OIW) because it is non-covalently bound in the hydration shells of charged molecules and ions, and therefore, not sufficiently mobile to join the growing ice crystals (Franks, 1986; Wolfe et al., 2002; Block, 2003). Although the phenomenon of insect freeze tolerance is widely recognized, the current knowledge about if and how the relative amount of ice fraction (IF) limits survival remains poor. Available data (summarized in Table S1) are mostly descriptive, although the relationship between IF and freeze tolerance was specifically addressed in some studies (Zachariassen, 1979;

Ramlov and Westh, 1993; Gehrken and Southon, 1997; Patricio Silva et al., 2013). Collectively, the literature suggests that seasonal change in the relative size of ice fraction may be one of the adaptive facets of the insect freeze-tolerance strategy (Block, 2003). A comprehensive test of such hypothesis, however, is missing.

In addition to the transition of liquid water into a crystalline phase – ice, we address in this study the transition into an amorphous non-crystalline solid – glass. The formation of amorphous glass 'traps' the structures and/or macromolecules and 'locks' them in place and conformation as they are at the moment of solidification. Until now, vitrification has been observed in only two cases in insects. The first evidence (Sformo et al., 2010) was obtained in larvae of the beetle *Cucujus clavipes puniceus*. These larvae avoid freezing by partial dehydration and concomitant accumulation of glycerol, which decreases their supercooling point to as low as -58°C. Some individuals, however, do not freeze at all (to at least -150°C), but vitrify. The second observation comes from partially frozen larvae of *Chymomyza costata* (Koštál et al., 2011b). It is known that the crystalline phase can coexist with the vitreous phase in partially frozen systems. At very low temperatures, and high concentrations of solutes in unfrozen phase, the residual solution may vitrify in presence of ice (Taylor et al., 2004). It should be noted that in medicinal cryobiology, the term vitrification is more often used to refer to a cryopresevation technique that attempts to vitrify the fully hydrated system without any ice formation (Fahy and Wowk, 2015), while dehydration or freeze concentration of body fluids played an important role in two insect examples.

Here we present results of thermal analysis of ice fraction dynamics during freezing of the larvae of two fly species using differential scanning calorimetry. In addition, we verify the occurrence and characterize the parameters of vitrification. The two fly models, *Chymomyza costata* and *Drosophila melanogaster* belong to the same family (Drosophilidae), their larvae are morphologically similar, and we sampled them at a relatively well defined and comparable ontogenetic stage. The larvae are ecologically similar during the warm season: growing and developing rapidly on decaying plant material. However, the two species inhabit different geographical regions; *D. melanogaster* originated in the tropics and has spread to mild temperate regions during the last century (Throckmorton, 1975), while *C. costata* lives in cool temperate and subarctic regions (Hackmann et al., 1970). Larvae of *D. melanogaster* do not overwinter, are highly chill-susceptible, and exhibit only mild capacity for cold-acclimation (Strachan et al.,

2011; Koštál et al., 2011a; 2012). In contrast, *C. costata* larvae are highly seasonal; these larvae overwinter in diapause and exhbibit extreme plasticity in freeze tolerance (Koštál et al., 2011b). By acclimating larvae of the two species at different photoperiods, temperatures, and dietary conditions, we were able to produce experimental variants that cover the whole conceivable range of insect freeze tolerances. Having these variants in hand, we asked the following specific questions: (i) Do ice fraction dynamics differ between the two species? (ii) Does acclimation affect ice fraction dynamics? (iii) Is there a maximum ice fraction that an insect can withstand? (iv) What is the effect of accumulated cryoprotectants, specifically proline, on ice fraction dynamics? (v) Do we see glass transition in both species and, if yes, under which conditions? (vi) Does vitrification correlate with survival of freezing?

MATERIALS and METHODS

Insects and acclimation treatments

Here we compared two dipterans with contrasting freeze tolerance capacities: the vinegar fly, *Drosophila* (*Sophophora*) *melanogaster*, and the malt fly, *Chymomyza costata* (Diptera: Drosophilidae). Cultures of vinegar flies (Oregon-R strain) and malt flies (Sapporo strain) were maintained in MIR 154 incubators (Sanyo Electric, Japan). Vinegar flies were reared as described earlier (Koštál et al., 2011a) on a standard cornmeal-yeast-agar diet, and malt flies were reared on a similar cornmeal-yeast-agar diet supplemented with ground malted barley (Lakovaara, 1969; Koštál et al., 2016b). All experiments were conducted with fully-grown 3rd instar larvae that were sampled from the diet prior to the onset of wandering behaviour. This ontogenetic stage was chosen because pre-wandering larvae can survive freezing of extracellular body fluids (Koštál et al., 2011b; 2012). To modulate the level of larval freeze tolerance, we applied different photoperiodic and thermal acclimation regimes, and augmented the diet with L-proline (Sigma-Aldrich, Saint Luis, MO, USA; abbreviated as proline hereon) as listed in Table 1.

In brief, all *D. melanogaster* larvae were grown under the same photoperiodic conditions: 12h/12h light/dark cycle (as larvae are photoperiodically insensitive); and one of three different thermal regimes (Table 1): constant 25°C (25), constant 15°C (15), and constant 15°C followed by 3 days at a fluctuating thermal regime of 6°C for 20h/11°C for 4h (FTR). Under FTR

conditions, *D. melanogaster* larvae enter quiescence (developmental arrest induced directly by low temperature) and increase their cold tolerance (Koštál et al., 2011a; 2016c). The larvae of *C. costata* reared under constant 18°C are photoperiodically sensitive; they continue direct development (to pupariation) under long days (16h/8h light/dark cycle, LD), but enter diapause (hormonally regulated developmental arrest) under short days (12h/12h light/dark cycle, SD; Koštál et al., 2000; 2016b). Gradual cold acclimation of diapausing (SD) larvae was performed by transferring them to 11°C and constant darkness at 6 weeks of age and, one week later, transferring them to 4°C for another 4 weeks. This cold acclimation (SDA) increases proline concentrations in the larvae and enhances freeze tolerance such that larvae survive cryopreservation in liquid nitrogen (LN_2) (Koštál et al., 2011b). We reared some larvae of both species on proline-augmented diets (50 mg proline per g standard diet, Pro50), which further increases freeze tolerance according to our previous studies (Koštál et al., 2011b; 2012; 2016a).

Freezing and cryopreservation protocols

The inoculation of larval body fluids with external ice crystals at relatively high sub-zero temperatures (close to 0°C) and slow cooling/freezing rates are two essential factors underlying survival in freezing assays (Shimada and Riihimaa, 1988). In our experiments, inoculative freezing was ensured by wrapping the larvae between two layers of moist cellulose, overlain with a small ice crystal (see Fig. S1 and Koštál et al., 2016a for a more detailed description). The standardization of all steps, including the cooling and warming rates, was achieved by performing all experiments in programmable Ministat 240 cooling circulators (Huber, Offenburg, Germany). Temperature inside the cellulose wrapping was monitored using K-type thermocouples connected to a PicoLog TC-08 datalogger (Pico Technology, St. Neots, UK).

The larvae of *D. melanogaster* show only limited ability to survive freezing and their freezing protocol was optimized previously (Koštál et al., 2012; 2016a). The optimal protocol (Fig. S2) consists of six steps: (i.) 20 min of manipulation with larvae at 0°C (washing larvae out of the diet, counting, placing into tubes); (ii.) 10 min of pre-incubation at -0.5°C (with ice crystal added); (iii.) slow cooling to -2°C for 180 min (cooling rate, 0.008°C min^{-1}); (iv.) rapid cooling to -5°C for 30 min; (v.) heating to +5°C for 40 min (heating rate, 0.25 °C min^{-1}); (vi.) melting at +5°C for 10 min.

The larvae of *C. costata* survive freezing relatively well and, when appropriatelly acclimated, can survive cryopreservation in LN_2 (Koštál et al., 2011b). In this study, we optimized the conditions of freezing and cryopreservation in SDA larvae by exposing them to protocols with modified rates and/or durations of cooling, heating, and incubation. A detailed description of all protocols is given in Table S2. The final optimum freezing/cryopreservation protocol for *C. costata* (Figs. S2, S3A) consisted of six steps: (i.) 20 min of larval manipulation at 0°C (washing larvae out of the diet, counting, placing into tubes); (ii.) slow cooling to -30°C (T_1) (with ice crystal added) for 300 min (cooling rate, r_1 = 0.1°C min^{-1}); (iii.) plunging into LN_2 for 60 min (or, alternatively, maintaining at T_1 for 60 min); (iv.) transferring from LN_2 to -30 °C (T_2); (v.) heating to +5°C for 60 min (heating rate, r_4 = 0.6 °C min^{-1}); (vi.) melting at +5°C for 10 min.

Freeze tolerance assays

The larvae of both species and all experimental variants (see Table 1) were exposed to optimal freezing protocols where the rates of cooling and heating were kept constant but the target temperatures (the minimum temperatures) varied. The data on freeze tolerance of *D. melanogaster* larvae were taken from our previous paper where the target temperatures varied between -2.5°C and -10°C (Koštál et al., 2016a; Table S3 A). Results for the freeze tolerance of *C. costata* larvae were obtained in the present study. The target temperatures for *C. costata* varied between -5°C and -75°C. Because our Ministats were not able to cool the larvae below -40°C, the freeze-tolerance assay at -75°C was conducted by pre-freezing the larvae to -40°C in Ministat and then transferring them to a freezer (Platinum 370H, Angelantoni, Massa Martana, Italy) where they gradually cooled to a temperature of -75°C (see the temperature record in Fig. S3B). After the end of freeze-tolerance assay, the unpacked cellulose balls were transferred to fresh standard diet in a tube maintained at constant 18°C. Alive/dead larvae were scored after 12 h recovery. All living larvae were maintained at 18°C for the subsequent 14 d (*D. melanogaster*) or 2 months (*C. costata*) and successful pupariation and emergence of adult flies were scored as criterions of survival. Exact numbers of larvae used for each specific experiment are shown in Results. Survival of cryopreservation in LN_2 was assessed in the SDA variant larvae of *C. costata* during the optimization of freezing and cryopreservation protocol (see above).

Differential scanning calorimetry

The dynamics of gradual ice fraction formation in a biological system is dictated by decreasing temperature according to a formula:

$$IF = OAW*(1 - (m.p./T)$$ (Wang and Weller, 2011),

meaning that the ice fraction (IF) is in equilibrium with osmolality (melting point, m.p. decreases 1.86°C per Osmol of dissolved osmotically active particles) at any given temperature (*T*), and the maximum ice fraction is limited by the amount of osmotically active water (OAW). In a real situation, this simple mathematical relationship is complicated by: (a) the supercooling capacity: a difference between the m.p. and the actual temperature of ice crystallization (supercooling point, T_{SCP}); (b) the activity of ice nucleators and/or anti-freeze proteins; and (c) the vulnerability of an insect to inoculation with external ice crystals (Zachariassen, 1985; Williams and Hirsch, 1986; Block, 1995).

We conducted the thermal analyses of whole larvae in 50 μL aluminum pans using a differential scanning calorimeter DSC4000 (Perkin Elmer, Waltham, MA, USA), with some modifications (will be described later) to previously described methods (Block, 1994; Koštál et al., 2011b). The temperature scale of the DSC was calibrated using indium and mercury according to the manufacturer's manual. The heat flow was calibrated by measuring the areas under the melt endotherms of known masses of ice (Fig. S4). We developed two different DSC protocols, abbreviated as *Equi-melt* (equilibrium melting) and *Ino-freeze* (inoculative freezing), to measure the latent heat absorbed/released during the first-order phase transitions (melting and freezing). Using these protocols, we analysed the relative IF size occurring in a partially frozen larva at a given sub-zero temperature.

In the *Equi-melt* protocol (Fig. S5), the larva was hermetically sealed in an aluminum pan and inserted into the DSC together with an empty reference aluminum pan. The larva was then rapidly cooled, and freezing occurred spontaneously at the larva's innate T_{SCP}. Maximum ice fraction (IF_{max}) was allowed to form as the larva reached sufficiently deep sub-zero temperature

(-30°C). Next, a portion of body ice was melted by heating the larva to a specific *Equi-melt* temperature (T_{EM}). The larva was equilibrated at T_{EM} for 30 min after which the remaining ice was melted. The equilibrium ice fraction for each specific T_{EM} was derived from melt endotherm and related to total body water (TBW). TBW was measured as a difference between total mass of the freshly sealed larva inside the aluminum pan and the total mass of the same pan, punctured after the DSC analysis and dried for 3 days at 60°C.

In the *Ino-freeze* protocol (Fig. S6), the pre-weighed larva was added into the instrument (placed into the aluminum pan that contained external ice crystals) during the run of a temperature programme, exactly at -1°C. The larva was inoculated with external ice crystals at a specific temperature (T_{INO}) and the ice fraction gradually increased during slow cooling/freezing at a rate of 0.1°C min^{-1} (simulating the conditions in freeze-tolerance assays) to a specific target temperature (used to analyze the presence/absence of vitrification; will be explained later). The amount of ice formed during the gradual freezing was estimated from the area under the freeze exotherm and related to TBW.

The thermal curves obtained by running the *Equi-melt* and *Ino-freeze* DSC protocols were analyzed using Pyris Software (Perkin Elmer) (see Figs. S5 and S6 for examples of analysis and more details). The fraction of freezable ('free'), osmotically active water (g OAW g^{-1} TBW) was calculated from the Boltzmann sigmoid curves fitted on summarized *Equi-melt* data. The fraction of unfreezable ('bound'), osmotically inactive water [(g OIW g^{-1} dry mass (DM)] was calculated analogously (Figs. S7 and S8).

The results of *Ino-freeze* protocols that were run with different target temperatures were used not only to derive the ice fraction from inoculative freeze exotherms, but also to observe (upon rapid heating) the occurrence and parameters of de-vitrification (de-glassing) phase transition (a second-order phase transition without absorbing/releasing any latent heat). Vitrification typically happens over a ca. 10°C temperature interval centered on a glass transition temperature (T_g) when the viscosity rises by a factor of 1,000, and heat capacity, thermal expansivity, and compressibility suddenly fall from liquid values to near those of a crystal (Wowk, 2010). Vitrified matter maintains the structure, energy and volume of a liquid, but the changes in energy and volume with temperature are similar in magnitude to those of a crystalline solid (Kauzmann, 1948). In this study, an inflection point of the de-glassing transition was read as the temperature of de-vitrification (T_{dg}). The specific change in heat capacity (*delta Cp*) was

derived from a difference in heat flow between the onset and the end of the de-glassing transition. The temperature of vitrification (T_g) during slow freezing (at a rate of 0.1°C min^{-1}) was estimated based on presence/absence of T_{dg} transition after reaching each specific target temperature of slow freezing (see Fig. S6 for more details).

Metabolomic analysis

Metabolomic analysis was performed for *C. costata* larvae only, while the comparative data for *D. melanogaster* were taken from our previous studies (Koštál et al., 2012; 2016a; c). Whole larvae of *C. costata* (pools of 5 larvae in each of 4 replicates) were sampled from the diet, weighed for fresh mass, plunged into liquid nitrogen, and stored at -80°C until analysis. The dry mass and water mass were measured in a parallel sample of 20 larvae weighed individually and dried at 65°C for 3 days. The pools of larvae were homogenized in 400 µl of methanol:acetonitrile:water mixture (volumetric ratio, 2:2:1) containing internal standards (*p*-fluoro-DL-phenylalanine, methyl α-D-glucopyranoside; both at a final concentration of 200 $nmol.ml^{-1}$; both from Sigma-Aldrich, Saint Luis, MI, USA). The TissueLyser LT (Qiagen, Hilden, Germany) was set to 50 Hz for 5 min (with a rotor pre-chilled to -20°C). Homogenization was repeated twice and the two supernatants from centrifugation at 20,000 g/5 min/4°C were combined. The extracts were subjected to targeted analysis of major metabolites using a combination of mass spectrometry-based analytical methods described previously (Koštál et al., 2016a; c).

Low-molecular-weight sugars and polyols were determined after *o*-methyloxime trimethylsilyl derivatization using a gas chromatograph (GC) with flame ionization detector GC-FID-2014 equipped with AOC-20i autosampler (both from Shimadzu Corporation, Kyoto, Japan). Profiling of acidic metabolites was done after the treatment with ethyl chloroformate under pyridine catalysis and simultaneous extraction in chloroform (Hušek and Šimek, 2001). The analyses were conducted using Trace 1300 GC combined with single quadrupole mass spectrometry (ISQ) (both from Thermo Fisher Scientific, San Jose, CA, USA) and liquid chromatograph Dionex Ultimate 3000 coupled with high resolution mass spectrometer Q Exactive Plus (all from Thermo Fisher Scientific). All metabolites were identified against relevant standards and subjected to quantitative analysis using a standard calibration curve method. All standards were purchased from Sigma-Aldrich. The analytical methods were

validated by simultaneously running blanks (no larvae in the sample), standard biological quality-control samples (the periodic analysis of a standardized larval sample – the pool of all samples), and quality-control mixtures of amino acids (AAS18, Sigma Aldrich).

RESULTS

Experimental variants cover the whole range of insect freeze tolerance

By exposing larvae of two drosophilid species to various acclimation conditions, we produced experimental variants that cover the broadest range of insect freeze tolerance: from intolerance (100% mortality) of mild freezing at -2.5°C for a few minutes in *D. melanogaster* larvae (variant 25) to almost 100% survival of larvae and high production of adults in *C. costata* (variant SDA) exposed to -75°C for a few hours (Fig. 1) or cryopreserved in LN_2 for 18 months (Table S2). The two species differed in the overall ability to tolerate freezing but, more importantly, we found that freeze tolerance is a highly plastic trait in both species. The actual level of freeze tolerance was strongly influenced by acclimation conditions (Fig. 1).

Ice fraction dynamics are similar among species and acclimation variants

We measured the ice fraction inside the larval body at different temperatures using two DSC-based methods. First, we measured the ice fraction that remains in the larval body after heating the frozen larva to T_{EM} (*Equi-melt* method). Boltzmann sigmoid curves fitted well to the empirical data (Figs. S7, S8), which allowed us to interpolate the ice fraction at any given temperature. The final curves describing the dynamisms of ice fraction formation at decreasing temperature for all experimental variants are presented in Fig. 2A, E. In the *Equi-melt* method, however, the ice crystals grow inside the larval body very rapidly at relatively low temperatures (at the larva's T_{SCP} ranging between approximately -16°C and -20°C). Freezing at the T_{SCP} is lethal in many insects including *C. costata* and *D. melanogaster* larvae. Therefore, we additionally used the *Ino-freeze* method to measure the ice fraction that gradually grows in the larval body after inoculative freezing at mild sub-zero temperatures (T_{INO}) (Figs. S9-S11). Both methods gave similar estimations of ice fraction (see overlap of *Equi-melt* lines and *Ino-freeze* ellipses in Fig. 2A, E). The two fly species and different experimental variants differed relatively

slightly (when compared to large differences in freeze tolerance) in various parameters of the ice fraction dynamics. Thus, the mean m.p. varied from -0.4°C to -1.0°C in *C. costata* variants, and from -0.4°C to -0.6°C in *D. melanogaster* variants. The IF_{max} varied between 67.9% and 76.1% of TBW in *C. costata* variants, and between 75.0 and 77.7% of TBW in *D. melanogaster* variants. The temperature at which 99% of IF_{max} was reached varied from -5.9°C to -10.5°C in *C. costata* variants, and from -3.9°C to -6.3°C in *D. melanogaster* variants (for details see Figs. S7, S8).

The two fly species differed in TBW, which ranged between 2.26 and 2.98 $mg.mg^{-1}$ DM in *C. costata* variants (Fig. 2B), and between 3.63 and 4.10 $mg.mg^{-1}$ DM in *D. melanogaster* variants (Fig. 2F). The OIW was relatively low in *C. costata* variants LD, SD and SDA (ranging between 0.67 and 0.85 $mg.mg^{-1}$ DM), while it was slightly higher in *C. costata* variant LD Pro50 and all variants of *D. melanogaster* (ranging between 0.90 and 0.96 $mg.mg^{-1}$ DM) (Figs. 2B, F). The inter-species difference in TBW was also reflected in the maximum ice content, which ranged between 1.5 and 2.3 $mg.mg^{-1}$ DM in *C. costata* variants (Fig. 2C), or between 2.7 and 3.2 $mg.mg^{-1}$ DM in *D. melanogaster* variants (Fig. 2G).

The association between ice fraction and freeze tolerance

Figure 3 shows the relationships between IF (derived from Fig. 2A, E and associated Figs. S7 and S8) and survival at a given sub-zero temperature (taken from Fig. 1). Three basic patterns were observed: (a) The freezing event was lethal (*D. melanogaster*, acclimation variants 25 and 15). (b) Lethal effects of freezing occured when the IF reached a specific threshold (*D. melanogaster*, acclimation variants 15 FTR and 15 FTR Pro50; *C costata*, acclimation variants LD and LD Pro50). The specific threshold for tolerable IF lay close to the IF_{max}, which corresponds to the OAW fraction (or, *vice versa*, which is limited by the OIW fraction). (c) The freezing event was always survived irrespective of the size of IF (*C. costata*, acclimation variants SD and SDA).

***Chymomyza costata* larvae accumulate high concentrations of proline**

We analyzed concentrations of 23 amino-compounds, 6 polyols, 3 sugars, 4 intermediates of the TCA cycle, and lactate (37 metabolites in total) in the larvae of *C. costata* (for details, see Table S3). The concentrations of the three most abundant metabolites (proline, glutamine, and

trehalose), plus the sum concentration of all other quantified metabolites, are presented in Fig. 2D. In order to make the direct comparison between two species, similar data for *D. melanogaster* are shown in Fig. 2H (Koštál et al., 2012; 2016a; c). The two species dramatically differed in their ability to accumulate proline. The larvae of *C. costata* naturally accumulated 339 mmol.kg^{-1} TBW of proline during cold acclimation (variant SDA). Feeding the non-diapause larvae of *C. costata* a proline-augmented diet (variant LD Pro50) increased the concentration of proline up to 487 mmol.kg^{-1} TBW. In contrast, *D. melanogaster* larvae naturally accumulated only 9 mmol.kg^{-1} TBW of proline (variant 15 FTR) and feeding them a proline-augmented diet increased the concentration of proline to only 57 mmol.kg^{-1} TBW (variant 15 FTR Pro50).

Glass transition occurs only in *Chymomyza costata*.

Vitrification (revealed as the presence of a de-glassing transition) was never registered in any DSC thermal analysis of *D. melanogaster* larvae (all experimental variants), irrespective of whether larvae were frozen rapidly (at the innate T_{SCP}) or gradually (after inoculation by external ice at T_{INO}), and irrespective of the target temperature (ranging between -5°C and -70°C). When heating frozen larvae back to 20°C at a fast rate of 10°C min^{-1}, typical melt endotherms were always observed, but characteristic de-glassing transition was absent in all cases.

In contrast, de-glassing transition was detected in DSC *Ino-freeze* thermal analyses of *C. costata* larvae for all experimental variants (see an example in Fig. S6). However, the presence/absence and parameters of de-glassing were strongly affected by acclimation and freezing conditions (Fig. 4). De-glassing never occurred in larvae that were frozen to target temperatures higher than -30°C. At the target temperature of -30°C, de-glassing transitions were observed only in SDA larvae (50% of cases) and LD Pro50 larvae (20% of cases) but not in LD or SD larvae. With decreasing target temperature, the frequency of T_{dg} transition occurrence rapidly increased in all experimental variants. Nevertheless, the rates of this increase differed among experimental variants in the order: SDA > LD Pro50 > SD > LD (Fig. 4A). Similar ordering of experimental variants was also observed in the other two parameters of de-glassing: T_{dg} and *delta Cp*. The mean T_{dg} varied from -15.8°C to -20.1°C and was variant-specific (SDA < LD Pro50 < SD < LD), but independent of target freezing temperature within each variant (slopes of linear regressions did not deviate from zero, Fig. 4B). The *delta Cp* was variant-specific (SDA

> LD Pro50 > SD > LD) and it increased as the target temperature decreased (slopes of linear regressions deviated from zero, Fig. 4C).

DISCUSSION

The differences in ice fraction dynamics among species and acclimation variants

We found that the ice fraction dynamics are closely similar in two drosophilid species [a response to our Introduction question (i)]. This close similarity contrasts to the profound differences observed in freeze tolerance between the two species. Temperature-dependent ice fraction dynamics in a larva is mathematically described by two partially interlocked parameters, the m.p. and OAW (Wang and Weller, 2011). As the m.p. ranged only moderately between -0.4 and -1.0°C in our study, its effect on ice fraction dynamics was relatively small (Figs. S7 and S8). The OAW affects the overall shape of ice fraction dynamics more profoundly, as it directly sets the IF_{max}. It is known that the total volume of OAW may undergo relatively massive and rapid changes in response to changing ambient conditions (Wharton and Worland, 2001; Block, 2002; Hadley, 2004), especially in small soil invertebrates that rely on the overwintering strategy of cryoprotective dehydration (Holmstrup and Westh, 1994). However, we did not see any dramatic changes in OAW in our model species. The OAW (IF_{max}) values measured in *D. melanogaster* and *C. costata* larvae, ranging between 67.9 and 77.7% TBW, fall withing the scope of published records for other insects, ranging between 64 and 84.5% TBW (Table S1).

The two model species differed mainly in their ability to phenotypically modulate IF_{max} in response to acclimation. [Introduction question (ii)]. The *C. costata* larvae showed decreases of IF_{max} upon entry into diapause, cold acclimation, and feeding on a proline-augmented diet. As discussed above, these shifts in IF_{max} were driven by concomitant decreases in m.p. and OAW fraction, both metrics intimately related to increasing osmolality of body fluids, which was driven by accumulation of proline. We will discuss later whether this phenotypic modulation of IF_{max} driven by proline may have some adaptive meaning. In contrast, the IF_{max} slightly increased in *D. melanogaster* larvae upon cold acclimation and entry into quiescence, while feeding on a proline-augmented diet had no effect on IF_{max}.

Increasing the OIW fraction has been proposed by Storey et al. (1981) as potentially important adaptive mechanism for insect freeze tolerance. They observed that warm-acclimated larvae of *Eurosta solidaginis* had 0.193 mg OIW.mg^{-1} DM, which considerably increased to 0.633 mg OIW.mg^{-1} DM after a 6-week stepwise acclimation to -30°C. The hypothesis about the adaptive meaning of increasing OIW rests fundamentally on concomitant reduction in OAW that causes reduction of IF at any given temperature and, consequently, mitigates the deleterious effects linked with freeze-induced cell dehydration. In this study, the OIW fraction was relatively constant in all acclimation variants in both species ranging between 0.67 and 0.96 mg.mg^{-1} DM. This amount of bound water was safely above the anhydrobiotic threshold of 0.2 – 0.4 mg.mg^{-1} DM that limits normal functionality of cellular structures and enzymes (Brovchenko and Oleinikova, 2008; Ball, 2008). Moreover, we have seen that the more freeze-tolerant larvae of *C. costata* exhibit a lower amount of OIW (expressed per mg DM) than the less freeze-tolerant larvae of *D. melanogaster*. These results lead us to question whether relatively small differences in OIW fraction explain such large variation in freeze tolerance in *C. costata* and *D. melanogaster* larvae.

The associations between ice fraction, unfreezable water, and freeze tolerance

The seemingly trivial question (iii) posed in Introduction: "Is there a maximum ice fraction that an insect can withstand?" appears as difficult to address empirically as it is to answer generally. Most likely, it is not the IF itself but rather the detrimental effects linked to freeze-induced dehydration, which limit the freeze tolerance. These effects include mechanical stress caused by growing extracellular ice crystals and shrinking of the cell, decreasing activity of water molecules, increasing ionic strength, acidity, concentrations of potentially toxic intermediates of metabolism, increasing viscosity and packing of macromolecules (Muldrew et al., 2004). The association between IF_{max}, OAW/OIW and larval survival is depicted in Fig. 3. Our data suggest that strongly freeze tolerant insects (such as cold-acclimated diapausing larvae of *C. costata*) survive after formation of IF_{max} inside their body. The maximum ice fraction that an insect can withstand thus obviously exists only for the insects falling into categories partial or moderate freeze tolerance [*sensu* Sinclair (1999), such as warm-acclimated active larvae of *C. costata* or quiescent and proline-fed larvae of *D. melanogaster*]. The existence of maximum tolerable IF

was previously estimated in other invertebrates (Zachariassen, 1979; Ramlov and Westh, 1993; Gehrken and Southon, 1997; Patricio Silva et al., 2013). However, the follow-up question on what mechanism sets this maximum tolerable IF remains open. We can only speculate why the maximum tolerable IF occurs relatively close to the IF_{max} not only in our study but also in the other studies: In adult tenebrionid beetles, *Eleodes blanchardi*, the IF_{max} represented approximately 75% TBW in both cold- and warm-acclimated specimens, which died when reaching a threshold IF of 62 and 65% TBW, respectively (Zachariassen, 1979). In New Zealand wetas, *Hemideina maori*, the IF_{max} was 82% TBW but they died when exposed to temperatures below -7°C which corresponds to approximately 81% TBW (Ramlov and Westh, 1993). In adult chrysomelid beetles, *Melasoma collaris*, the IF_{max} varied between 77 and 84.5% TBW (cold- and warm-acclimated, respectively), and the lower limit of freeze tolerance was associated with the IF of 73-75% TBW (Gehrken and Southon, 1997). In a freeze-tolerant potworm, *Enchytraeus albidus*, the IF was manipulated by exposing them to various sub-zero temperatures and environmental salinities. For two different populations of potworms, it was found that lethal effects of freezing occurred when the relative ice fraction reached a sharp threshold between 56% and 57% TBW while the IF_{max} was similar in both populations, 58.8 and 61.4% TBW, respectively (Patricio Silva et al., 2013). One potential hypothetical explanation for such commonality (proximity of maximum tolerable IF to IF_{max}) could be that some (moderately) freeze-tolerant insects can tolerate the loss of most of their OAW relatively well, while greater losses impair the integrity of the OIW pool and, consequently, lead to irreversible changes in macromolecular conformation (Wang, 1999; Ball, 2008; Brovchenko and Oleinikova, 2008) and ultimately mortality. Other (partially) freeze-tolerant insects can be sensitive to even relatively small losses of their OAW associated with relatively mild cell dehydration.

Cryoprotective roles of accumulated proline

In response to our Introduction question (iv) on effects of proline on ice fraction, we can say that in both fly species the accumulated proline affected the empirically-measured parameters of ice fraction dynamics according to its theoretically-expected colligative effects on biological systems. The m.p., the relative OAW fraction, and the IF_{max}, all decreased with increasing proline concentration. The classically-proposed mechanistic model of cryoprotection is based just on these colligative effects. This model posits that at any given cryogenic temperature *T*, the amount

of extracellular ice and, consequently, the magnitude of deleterious cellular freeze-dehydration, is lower in the system with accumulated cryoprotectant than in the system without cryoprotectant (Lovelock, 1954; Salt, 1961; Meryman, 1971; Zachariassen, 1985; Storey and Storey, 1988; Lee, 2010). Our results suggest that the colligative effects linked to proline accumulation are detectable in fly larvae and may thus theoretically contribute to larval freeze tolerance. However, these colligative effects should not be used as sole and straightforward predictors of freeze tolerance. The insect cold tolerance literature agrees on a view that a single molecule, such as proline, may play more than one (colligative) mechanistic role in building the insect's freeze tolerance. Moreover, a whole complex of other mechanisms, in addition to accumulation of cryoprotectants, needs to be taken into account in order to fully explain the resulting freeze tolerance (for review, see Storey and Storey 1988; 1991; Sinclair, 1999; Lee; 2010).

We are of the view that proline exerts its protective role in *C. costata* by a combination of mechanisms, and that the importance of individual mechanisms may gradually change with the acclimation state of the insect during the course of its entry into dormancy, cold acclimation, cooling, and freezing. Thus, proline might be actively involved in entry into diapause via its diverse regulatory functions in sensing the energy status and production of reactive oxygen species (Phang et al., 2010; Liang et al., 2013). Proline can also scavenge free radicals (Kaul et al. 2008). Proline accumulation continues as the ambient temperature decreases. Finally, proline levels elevate to 339 mmol.kg^{-1} TBW in cold-acclimated, diapausing larvae (*C. costata*, SDA variant), which represents as much as 499 mmol.kg^{-1} OAW. Our previous analysis (Koštál et al., 2011b) most probably under-estimated the concentration of proline in cold-acclimated *C. costata* larvae (showing only 147 mmol.kg^{-1} TBW). The higher value (339 mmol.kg^{-1} TBW) is correct, as we have verified in several generations of larvae since the original publication. It is plausible to propose that at this high concentration proline helps to reduce partial unfolding of proteins in chilled and supercooled larvae (prior to freezing) via the mechanism of preferential exclusion (Arakawa and Timasheff, 1985; Timasheff, 1992; 2002; Bolen and Baskakov, 2001). Upon freezing, proline can serve as a molecular shield and prevent aggregation of partially unfolded proteins or fusion of membranes in tightly packed organelles (Bryant et al., 2001; Hoekstra et al., 2001; Hoekstra and Golovina, 2002; Ball, 2008). Upon reaching high levels of freeze-dehydration, proline concentrations exceed > 1 mol kg^{-1} TBW. At such extremely high concentrations, proline is known to form specific supramolecular aggregates (Rudolph and

Crowe, 1986; Samuel et al., 2000) which may interact with the hydrophobic surfaces presented by partially unfolded proteins, thereby stabilizing the folding intermediates and preventing their aggregation (Samuel et al., 1997; Ignatova and Gierasch, 2006; Das et al., 2007). In addition, the supramolecular structures of proline may promote the formation of amorphous biological glass – vitrification (Rudolph and Crowe, 1986).

The association between glass transition and freeze tolerance

We observed glass transition in all acclimation variants of *C. costata* but found no indication of glass transition in *D. melanogaster* larvae [Introduction question (v.)]. Our study provides no direct mechanistic explanation for why this difference between two species exists. Although proline is known to stimulate glass transition (Rudolph and Crowe, 1986), we assume that some additional mechanisms should be involved in stimulation of glass transition in *C. costata* (compare: no glass transition in *D. melanogaster*, variant 15 FTR Pro50 (proline, 57.2 mmol.kg-1 TBW) *vs.* T_{dg} ~ -17°C in *C. costata*, variant LD (proline, 31.4 mmol.kg-1 TBW).

We found that de-vitrification occurs around -20°C, while vitrification is completed in all larvae of the SDA variant of *C. costata* at approximately -30°C (Fig. 5). Interestingly, we found that these larvae can survive plunging into LN_2 only when slowly pre-frozen to below -20°C (corresponding to T_{dg}), and that they can survive and metamorphose into adults only when slowly pre-frozen to below -30°C (corresponding to a completion of glass transition). Assuming that T_g must lie somewhere in the interval between T_{dg} and the completion of glass transition, our results reveal a strikingly tight association between glass transition and dramatic increase of survival of cryopreserved SDA *C. costata* larvae (Fig. 5). Based on these results, we formulate the answer to our last Introduction question (vi): the correlative evidence was obtained showing that vitrification of the residual solution after formation of IF_{max} is associated with the survival of SDA *C. costata* larvae cryopreserved in LN_2. We suggest that vitrification may further stabilize the structures of macromolecular complexes and protect them against thermomechanical stress (Rubinsky et al., 1980) linked to rapid changes of temperature during plunging into LN_2 and re-warming.

CONCLUSIONS

Using DSC thermal analysis, we found that temperature-dependent ice fraction dynamics are closely similar in the larvae of *D. melanogaster* and *C. costata* (each species analyzed in four different acclimation variants). The two species differed mainly in their ability to phenotypically modulate the parameters of ice fraction dynamics in response to acclimation. The *C. costata* larvae decreased m.p., OAW, and IF_{max} upon entry into diapause, cold acclimation, and feeding on a proline-augmented diet. The maximum tolerable IF changed accordingly to the acclimation state in both species: from freeze intolerance to a specific threshold (partial freeze tolerance) in *D. melanogaster*, or from a specific threshold to independence of IF (strong freeze tolerance) in *C. costata*. The specific threshold (maximum tolerable IF) was situated very close to IF_{max}. The phenotypic shifts in ice fraction dynamics were associated with colligative effects caused by accumulated proline. In addition to colligative effects, accumulated proline likely affected freeze tolerance of *C. costata* larvae by a combination of other mechanisms. We have not detected any glass transitions in *D. melanogaster* larvae exposed to temperatures as low as -70°C. In contrast, the glass transitions of the residual solution after formation of IF_{max} occurred at temperatures below -30°C in all acclimation variants of *C. costata.* We found a tight correlation between the occurrence of glass transition and dramatic increase of survival in LN_2-cryopreserved *C. costata* larvae of the acclimation variant SDA.

ACKNOWLEDGEMENTS

We thank Irena Vacková, Anna Heydová, Iva Opekarová, and Helena Zahradníčková (all from Biology Centre CAS) for assistance with insect rearing, sample preparation and analyses. We thank Lauren Des Marteaux (Biology Centre CAS) for commenting on an early version of the paper.

COMPETING INTERESTS

No competing interests declared.

AUTHOR CONTRIBUTIONS

Jan Rozsypal and Vladimír Koštál designed the research. Jan Rozsypal conducted the experiments. Martin Moos and Petr Šimek performed the metabolomic analysis. Vladimír Koštál wrote the manuscript. All authors read and approved the paper.

FUNDING

This work was supported by Czech Science Foundation grant 16-06374S (to V.K.).

REFERENCES

Arakawa, T. and Timasheff, S.N. (1985). The stabilization of proteins by osmolytes. *Biophys. J.* **47**, 411-414.

Asahina, E. (1969). Frost resistance in insects. *Adv. Insect Physiol.* **6**, 1-49.

Bale, J.S. (1993). Classes of insect cold hardiness. *Funct. Ecol.* **7**, 751-753.

Bale, J.S. (1996). Insect cold hardiness: A matter of life and death. *Eur. J. Entomol.* **93**, 369-382.

Ball, P. (2008). Water as an active constituent in cell biology. *Chem. Rev.* **108**, 74-108.

Block, W. (1994). Differential scanning calorimetry in ecophysiological research. *Acta Oecol.* **15**, 13-22.

Block, W. (1995). Insects and freezing. *Sci. Progr.* **78**, 349-372.

Block, W. (2002). Interactions of water, ice nucleators and desccation in invertebrate cold survival. *Eur. J. Entomol.* **99**, 259-266.

Block, W. (2003). Water or ice? – the challenge for invertebrate cold survival. *Sci. Progr.* **86**, 77-101.

Block, W., Bauer, R. (2000). DSC studies of freezing in terrestrial enchytraeids (Annelida: Oligochaeta). *CryoLett.* **21**, 99-106.

Block, W., Wharton, D.A., Sinclair, B.J. (1998). Cold tolerance of a New Zealand alpine cockroach, *Celatoblatta quinquemaculata*. *Physiol. Entomol.* **23**, 1-6.

Bolen, D.W. and Baskakov, I.V. (2001). The osmophobic effect: natural selection of a thermodynamic force in protein folding. *J. Mol. Biol.* **310**, 955-963.

Brovchenko, I. and Oleinikova, A. (2008). Which properties of a spanning network of hydration water enable biological functions? *Chem. Phys. Chem.* **9**, 2695-2702.

Bryant, G., Koster, K.L. and Wolfe, J. (2001). Membrane behaviour in seeds and other systems at low water content: the various effects of solutes. *Seed Sci. Res.* **11**, 17-25.

Das, U., Hariprasad, G., Ethayathulla, A.S., Manral, P., Das, T.K., Pasha, S., Mann, A., Ganguli, M., Verma, A.K., Bhat, R., Chandrayan, S.K., Ahmed, S., Sharma, S., Kaur, P., Singh, T.P. and Srinivasan, A. (2007). Inhibition of protein aggregation: Supramolecular assemblies of arginine hold the key. *PLoS One* **11**, e1176.

Duman, J.G. (2001). Antifreeze and ice nuclator proteins in terrestrial arthropods. *Annu. Rev. Physiol.* **63**, 327-357.

Duman, J.G. (2015). Animal ice-binding (antifreeze) proteins and glycolipids: an overview with emphasis on physiological function. *J. Exp. Biol.* **218**, 1846-1855.

Fahy, G.M., Wowk, B. (2015). Principles of cryopreservation by vitrification. *Methods Mol. Biol.* **1257**, 21-82.

Franks, F. (1986). Unfrozen water: yes; unfreezable water: hardly; bound water: certainly not. An editorial note. *CryoLett.* **7**, 207.

Gehrken, U., Southon, T.E. (1997). Effect of temperature on cold-hardiness and tissue ice formation in the adult chrysomelid beetle Melasoma collaris L. *J. Insect Physiol.* **43**, 587-593.

Hackmann, W., Lakovaara, S., Saura, A., Sirsa, M., Vepsalainen, K. (1970). On the biology and karyology of *Chymomyza costata* Zetterstedt, with reference to the taxonomy and distribution of various species of *Chymomyza* (Dipt., Drosophilidae). *Ann. Ent. Fenn.* **36**, 1-9.

Hadley, N.F. (1994). *Water Relations of Terrestrial Arthropods.* Academic Press, San Diego.

Halberg, K.A., Persson, D., Ramlov, H., Westh, P., Kristensen, R.M., Mobjerg, N. (2009). Cyclomorphosis in Tardigrada: adaptation to environmental constraints. *J. Exp. Biol.* **212**, 2803-2811.

Hengherr, S., Worland, M.R., Reuner, A., Brümmer, F, Schill, R.O. (2009). Freeze tolerance, supercooling points and ice fromation: comparative studies on the subzero temperature survival og limno-terrestrial tardigrades. *J. Exp. Biol.* **212**, 802-807.

Hoekstra, F.A., Golovina, E.A. (2002). The role of amphiphiles. *Comp. Biochem. Physiol. A* **131**, 527-533.

Hoekstra, F.A., Golovina, E.A., Buitink, J. (2001). Mechanisms of plant desiccation tolerance. *Trends Plant Sci.* **6**, 431-438.

Holmstrup, M., Bayley, M., Ramlov, H. (2002). Supercool or dehydrate? An experimental analysis of overwintering strategies in small permeable arctic invertebrates. *Proc. Natl. Acad. Sci. USA* **99**, 5716-5720.

Holmstrup, M., Westh, P. (1994). Dehydration of earthworm eocoons exposed to cold – a novel cold-hardiness mechanism. *J. Comp. Physiol. B* **164**,312-315.

Hušek, P., Šimek, P. (2001). Advances in amino acid analysis. *LC-GC North Am.* **19**, 986-999.

Ignatova, Z. and Gierasch, L.M. (2006). Inhibition of protein aggregation in vitro and in vivo by a natural osmoprotectant. *Proc. Natl. Acad. Sci. USA* **103**, 13357-13361.

Kaul, S., Sharma, S.S., Mehta, I.K. (2008). Free radical scavenging potential of L-proline: evidence from in vitro assays. *Amino Acids* **34**, 315-320.

Kauzmann, W. (1948). The nature of the glassy state and the behavior of liquids at low temperatures. *Chem. Rev.* **43**, 219-256.

Koštál,V., Korbelová, J., Poupardin, R., Moos, M., Šimek, P. (2016a). Arginine and proline applied as food additives stimulate high freeze tolerance in larvae of *Drosophila melanogaster*. *J. Exp. Biol.* **219**, 2358-2367.

Koštál,V., Korbelová, J., Rozsypal, J., Zahradníčková, H., Cimlová, J., Tomčala, A. and Šimek P. (2011a). Long-term cold acclimation extends survival time at 0°C and modifies the metabolomic profiles of the larvae of the fruit fly *Drosophila melanogaster*. *PLoS One* **6**, e25025.

Koštál, V., Korbelová, J., Štětina, T., Poupardin, R., Colinet, H., Zahradníčková, H., Opekarová, I., Moos, M., Šimek, P. (2016c). Physiological basis for low-temperature survival and storage of quiescent larvae of the fruit fly *Drosophila melanogaster. Sci. Rep.* **6**, 32346.

Koštál, V., Mollaei, M., Schöttner, K. (2016b). Diapause induction as an interplay between seasonal token stimuli, and modifying and directly limiting factors: hibernation in *Chymomyza costata. Physiol. Entomol.* **41**, 344-357

Koštál, V., Shimada K., Hayakawa Y. (2000). Induction and development of winter larval diapause in a drosophilid fly, *Chymomyza costata*. *J. Insect Physiol.* **46**, 417-428.

Koštál, V., Šimek, P., Zahradníčková, H., Cimlová, J. and Štětina T. (2012). Conversion of the chill susceptible fruit fly larva (*Drosophila melanogaster*) to a freeze tolerant organism. *Proc. Natl. Acad. Sci. USA* **109**, 3270-3274.

Koštál, V., Zahradníčková, H. and Šimek, P. (2011b). Hyperprolinemic larvae of the drosophilid fly, *Chymomyza costata*, survive cryopreservation in liquid nitrogen. *Proc. Natl. Acad. Sci. USA* **108**, 13035-13040.

Lakovaara, S. (1969). Malt as a culture medium for *Drosophila* species. *Drosoph. Inf. Serv.* **44**,128.

Lee Jr., R.E. (2010). A primer on insect cold-tolerance. In *Low Temperature Biology of Insects* (ed. D.L. Denlinger, D.L. and R.E. Lee), pp. 3-34. Cambridge: Cambridge University Press.

Lee Jr., R. E., Lewis E. A. (1985), Effect of temperature and duration of exposure on tissue ice formation in the gall fly *Eurosta solidaginis* (Diptera, Tephritidae). *Cryo-Lett.* **6**, 25-34.

Liang, X., Zhang, L., Natarajan, S.K., Becker, D.F. (2013). Proline mechanisms of stress survival. *Antiox. Redox Signal.* 19**, 998-1011.**

Lovelock, J.E. (1954). The protective action of neutral solutes against haemolysis by freezing and thawing. *Biochem. J.* **56**, 265-270.

Meryman, H.T. (1971). Osmotic stress as a mechanism of freezing injury. *Cryobiol.* **8**, 489-500.

Muldrew, K., Acker, J.P., Elliott, J.A.V., McGann, L.E. (2004). The water to ice transition: Implications for living cells. In *Life in the Frozen State* (ed. B. Fuller, N. Lane, E.E. Benson), pp. 67-108. Boca Raton: CRC Press.

Phang, J.M., Liu, W., Zabirnyk, O. (2010). Proline metabolism and microenvironmental stress. *Annu. Rev. Nutr* . **30**, 441-463.

Ramlov, H., Westh, P. (1993). Ice formation in the freeze-tolerant Alpine weta *Hemideina maori* Hutton (Orthoptera, Stenopelmatidae). *Cryo-Lett*. **14**, 169-176.

Renault, D., Salin, C., Vannier, G., Vernon, P. (2002). Survival at low temperatures in insects: What is the ecological significance of the supercooling point? *CryoLett.* **23**, 217-228.

Rubinsky, B., Cravalho, E.G., Mikic, B. (1980). Thermal stress in frozen organs. *Cryobiol.* **17**, 66-73.

Rudolph, A.S. and Crowe, J.H. (1986). A calorimetric and infrared spectroscopic study of the stabilizing solute proline. *Biophys. J.* **50**, 423-430.

Salt, R.W. (1961). Principles of insect cold-hardiness. *Annu. Rev. Entomol.* **6**, 55-74.

Samuel, D., Kumar, T.K.S., Ganesh, G., Jayaraman, G., Yang, P.W., Chang, M.M., Trivedi, W.D., Wang, S.L., Hwang, K.C., Chang, D.K. and Yu, C. (2000). Proline inhibits aggregation during protein refolding. *Prot. Sci.* **9**, 344-352.

Samuel, D., Kumar, T.K.S., Jayaraman, G., Yang, P.W. and Yu, C. (1997). Proline is a protein solubilizing solute. Biochem. *Mol. Biol. Int.* **41**, 235–242.

Sformo, T., Walters, K., Jeannet, K., Wowk, B., Fahy, G.M., Barnes, B.M., Duman, J.G. (2010). Deep supercooling, vitrification and limited survival to -100°C in the Alaskan

beetle *Cucujus clavipes puniceus* (Coleoptera: Cucujidae) larvae. *J. Exp. Biol.* **213**, 502-509.

Shimada, K., Riihimaa, A. (1988). Cold acclimation, inoculative freezing and slow cooling: essential factors contributing to the freezing-tolerance in diapausing larvae of *Chymomyza costata* (Diptera: Drosophilidae). *CryoLett.* **9**, 5-10.

Sinclair, B.J. (1999). Insect cold tolerance: How many kinds of frozen? *Eur. J. Entomol.* **96**, 157-164.

Sinclair, B.J., Renault, D. (2010). Intracellular ice formation in insects: Unresolved after 50 years? *Comp. Biochem. Physiol. A* **155**, 14-18.

Sinclair, B.J., Vernon, P., Klok, C.J., Chown, S.L. (2003). Insects at low temperatures: an ecological perspective. *Trends Ecol. Evol.* **18**, 257-262.

Somme, L. (1982). Supercooling and winter survival in terrestrial arthropods. *Comp. Biochem. Physiol.* **A73**, 519-543.

Storey, K.B., Baust, J.G., Bueschner, P. (1981). Determination of water "bound" by soluble subcellular components during low-temperature acclimation in the gall fly larva, *Eurosta solidaginis*. *Cryobiol.* **18**, 315-321.

Storey, K.B., Storey, J.M. (1988). Freeze tolerance in animals. *Physiol. Rev.* **68**, 27-84.

Storey, K.B., Storey, J.M. (1991). Biochemistry of cryoprotectants. In *Insects at Low Temperature* (R.E. Lee and D.L. Denlinger), pp. 64-93. New York and London: Chapman and Hall.

Strachan, L.A., Tarnowski-Garner, H.E., Marshall, K.E., Sinclair, B.J. (2011). The evolution of cold tolerance in *Drosophila* larvae. *Physiol. Biochem. Zool.* **84**, 43-53.

Taylor, M.J., Song, Y.C., Brockbank, K.G.M. (2004). Vitrification in tissue preservation: new developments. In *Life in the Frozen State* (ed. B. Fuller, N. Lane, E.E. Benson), pp. 603-641. Boca Raton: CRC Press.

Throckmorton, L.H. (1975). The phylogeny, ecology, and geography of *Drosophila*. In *Handbook of Genetics: Invertebrates of Genetic Interest.* (ed. R.C. King), pp. 421-469. New York: Plenum.

Timasheff, S.N. (1992). A physicochemical basis for the selection of osmolytes by nature. In *Water and Life: A Comparative Analysis of Water Relationships at the Organismic,*

Cellular, and Molecular Levels (ed. G.N. Somero, C.B. Osmond and C.L. Bolis), pp. 70-84. Berlin: Springer Verlag.

Timasheff, S.N. (2002). Protein-solvent preferential interactions, protein hydration, and the modulation of biochemical reactions by solvent components. *Proc. Natl. Acad. Sci. USA* **99**, 9721-9726.

Wang, L., Weller, C.L. (2011). Thermophysical properties of frozen foods. In *Handbook of Frozen Food Processing and Packaging*, 2nd edition (ed. D.-W. Sun), pp. 101-125. Boca Raton: CRC Press.

Wang, W. (1999). Instability, stabilization, and formulation of liquid protein pharmaceuticals. *Internatl. J. Pharm.* **185**, 129-188.

Westh, P. and Kristensen, R. M. (1992). Ice formation in the freeze-tolerant eutardigrades *Adorybiotus coronifer* and *Amphibolus nebulosus* studied by differential scanning calorimetry. *Polar Biol.* **12**, 693- 699.

Wharton, D.A., Ferns, D.J. (1995). Survival of intracellular freezing by the antarctic nematode *Panagrolaimus davidi. J. Exp. Biol.* **198**, 1381-1387.

Wharton, D. A., Block, W. (1997). Differential scanning calorimetry studies on an Antarctic nematode (*Panagrolaimus davidi*) which survives intracellular freezing. *Cryobiol.* **34**, 114–121.

Wharton, D.A., Worland, M.R. (2001), Water relations during desiccation of cysts of the potato-cyst nematode *Globodera rostochiensis*. *J. Comp. Physiol. B* **171**, 121-126.

Williams, R.J., Hirsch, A.G. (1986). On the freezing of water and the melting of ice in scanning calorimeters. *CryoLett* **7**, 146-161.

Wolfe, J., Bryant, G, Koster, K.L. (2002). What is "unfreezable water", how unfreezable is it and how much is there? *CryoLett.* **23**, 157-166.

Worland, M.R., Block, W., Grubor-Lajsic, G. (2000). Survival of *Heleomyza borealis* (Diptera, Heleomyzidae) larvae down to -60°C. *Physiol. Entomol.* **25**, 1-5.

Wowk, B. (2010). Thermodynamic aspects of vitrification. *Cryobiol.* **60**, 11-22.

Zachariassen, K.E. (1985). Physiology of cold tolerance in insects. *Physiol. Rev.* 65, 799-832.

Zachariassen, K.E., Hammel, H.T., Schmidek, W. (1979). Osmotically inactive water in relation to tolerance to freezing *in Eleodes blanchardi* beetles. *Comp. Biochem. Physiol. A* **63**, 203-206.

Zachariassen, K.E., Kristiansen, E. (2000). Ice nuclation and antinucleation in nature. *Cryobiol.* **41**, 257-279.

Figures

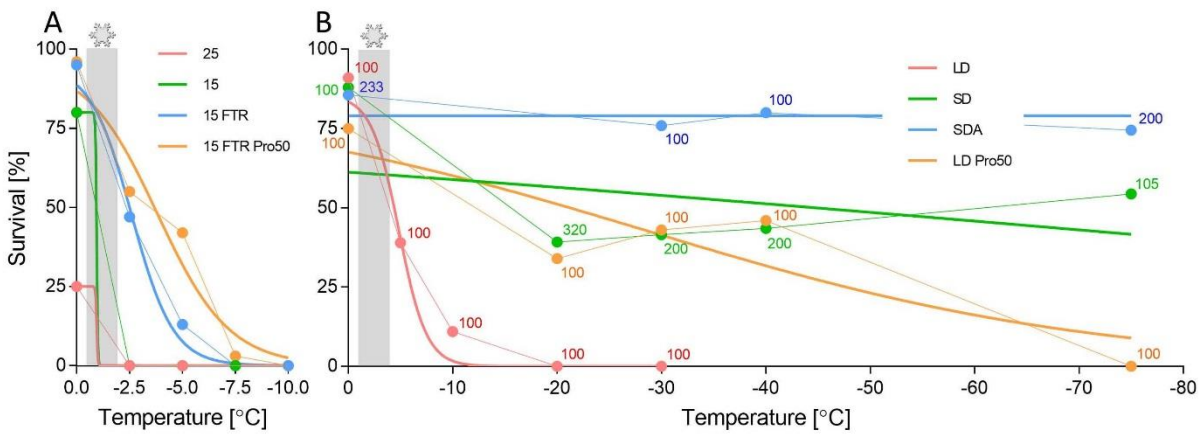

Fig. 1. Larval freeze tolerance in two drosophilid fly species.

Prior to freeze-tolerance assays, larvae were maintained under different acclimation conditions (see Table 1) in order to induce variation in freeze tolerance. During the assays, the larval body fluids were seeded by external ice crystals and gradually cooled to a target temperature (*x* axis) at a slow rate (see Figs. S1-S3 for more details). After thawing, the larvae were returned to artificial diets and their ability to metamorphose into the adult stage was used as a criterion for survival. (A) *Drosophila melanogaster*, data are taken from our previous paper (Koštál et al., 2016a; Table S3 A). (B) *Chymomyza costata*, original data obtained in the present study. Numbers flanking the datapoints show the numbers of larvae exposed to each temperature.

Sigmoid curves were fitted to all data: Y=Bottom + (Top-Bottom)/(1+10^((LogEC50-X)*HillSlope)), where bottom is constrained to 0, and Top is constrained to survival of controls exposed at 0°C for 20 min (manipulation time).

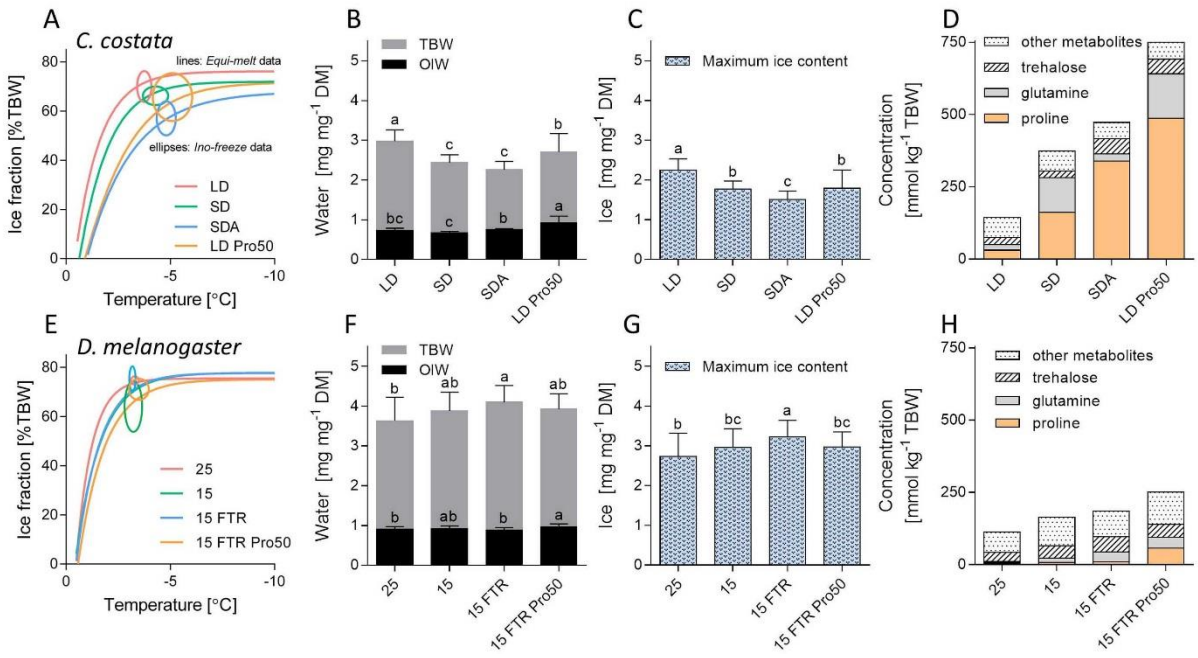

Fig. 2: Ice fraction dynamics and related parameters in larvae of two drosophilid fly species.

(A-D, *Chymomyza costata*; E-H, *Drosophila melanogaster*). The larvae were maintained under different acclimation conditions and exhibited different levels of freeze tolerance (see Fig. 1). (A, E) The gradual increase of ice fraction with decreasing temperature was measured using two variants of the DSC technique: Boltzmann sigmoids were fitted to *Equi-melt* data and ellipses were based on mean $x \pm$ S.D. and mean $y \pm$ S.D. values of *Ino-freeze* data (see text and Figs. S5 and S6 for more details). (B, F) Total body water (TBW) content and the amount of unfreezable, osmotically inactive water (OIW). (C, G) The maximum ice content calculated as the difference between TBW and OIW. (D, H) Summary of metabolomic analyses. The three most abundant metabolites are shown: proline, glutamine, and trehalose. The remaining 34 quantified metabolites are shown only as a sum of other metabolites. The data for *Chymomyza costata* were obtained in the present study (see Table S3 for more details), while the data for *Drosophila melanogaster* are taken from our previous studies (Koštál et al., 2012; 2016a; 2016c). The means (columns) in (B, C, F, G) flanked by different letters are significantly different according to ANOVA followed by Bonferroni's post hoc test. See Figs. S7-S10 for complete datasets.

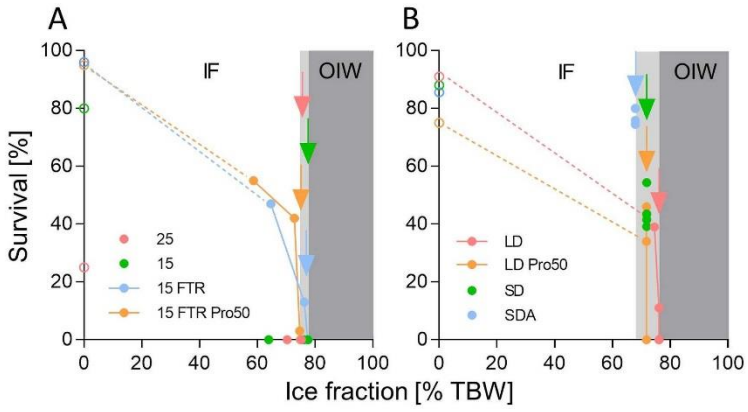

Fig. 3. Association between ice fraction and freeze tolerance.

Data on survival (Fig. 1) plotted against data on ice fraction (Fig. 2A, E) for (A) *Drosophila melanogaster* and (B) *Chymomyza costata* larvae. The grey areas show the fraction of unfreezable, osmotically inactive water (OIW). The pale grey part delimits the range of OIW differences among acclimation variants. Colored arrows show the exact position of a boundary between OIW and fraction of osmotically active water (here shown as maximum ice fraction, IF_{max}) for individual acclimation variants. The dashed lines are used to visually connect the datapoints to the respective initial values (survival after exposure to 0°C for 20 min).

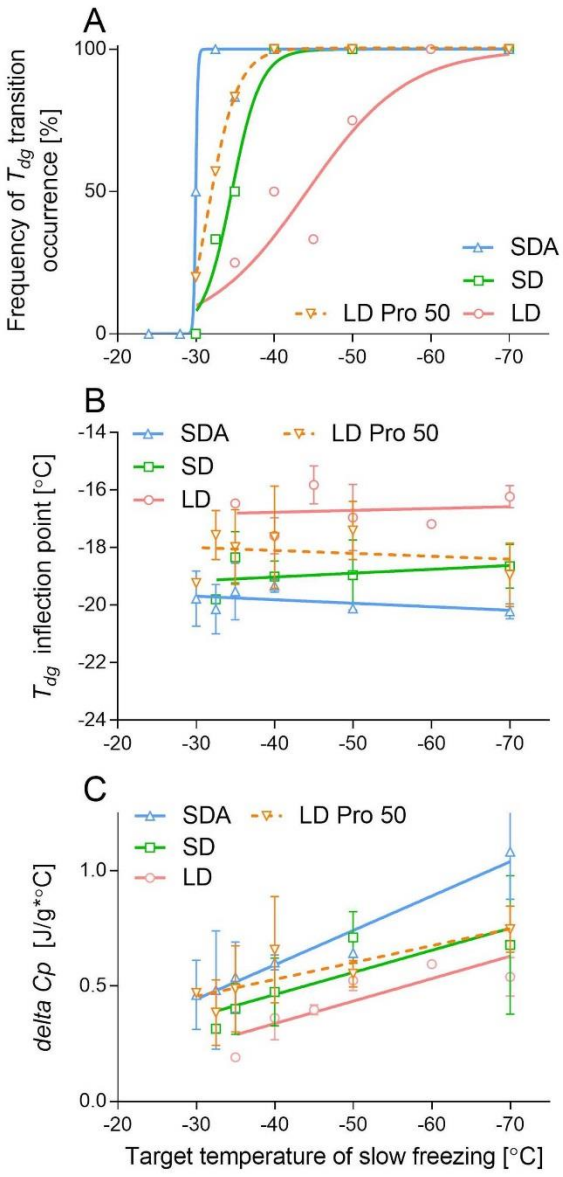

Fig. 4. De-glassing transition analysis in *Chymomyza costata*.

Larvae were maintained under different acclimation conditions and exhibited different levels of freeze tolerance (see Fig. 1). (A, B) The inflection point of the de-glassing transition was read as the temperature of de-vitrification (T_{dg}). (C) The specific change in heat capacity (*delta Cp*) was derived from a difference in heat flow between the onset and the end of the de-glassing transition. In (A), each point is a percentage of larvae showing the de-vitrification transition after freezing to

different target temperatures (see Fig. S6). In (B, C), each point is a mean ± S.D. of several larvae (see text and Fig. S11 A for details).

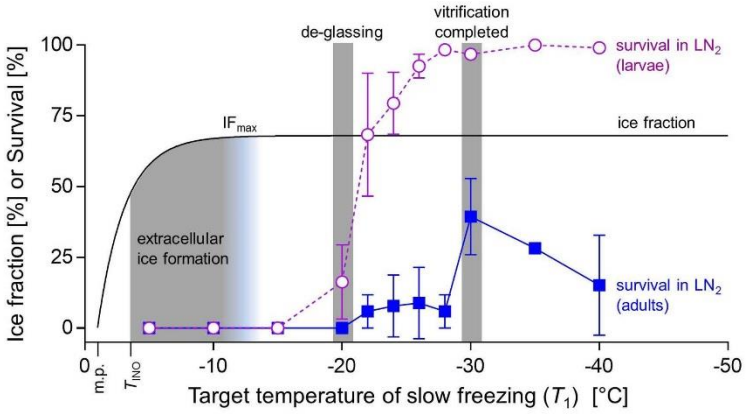

Fig. 5. Summary of data for cold-aclimated, diapausing larvae of *Chymomyza costata*.

The graph integrates results on gradually growing body ice fraction with decreasing temperature (black solid line, the same Boltzmann curve as shown in Fig. S7 C), survival after cryopreservation in LN_2 (see below for explanation), and depicts several important transitions: the melting point (m.p.) derived from the Boltzmann curve is -1°C; the larvae are inoculated with external ice crystals at -2.6°C on average (T_{INO}, Fig. S1 F), and 99% of maximum ice fraction (IF_{max}) is formed at -10.5°C (Fig. S7C). The larvae exhibit the de-vitrification transition (upon warming) at approximately -20°C (Fig. 3 B) but their vitrification is not completed (not observable by de-vitrification signal) at temperatures higher than -30°C (Fig. 3 A). Note the association between the vitrification transition (occurring between de-glassing and vitrification completed temperatures) and the steep increase in survival of larvae and adults in the cryopreservation conditions (LN_2). Survival lines show the same data as presented in Table S2, where the target temperature of slow freezing (T_1, just prior to plunging into LN_2) is variable.

Table 1: Photoperiodic, thermal, and dietary conditions used to induce different levels of freeze tolerance in larvae of *Drosophila melanogaster* and *Chymomyza costata*.

Species	Treatment	Photoperiod [light/dark]	Temperature (time)**	Diet
D. melanogaster	25	12h/12h	25°C (5d)	standard
	15	12h/12h	15°C (11d)	standard
	15 FTR	12h/12h	15°C (11d) → 6°C /11°C (3d)	standard
	15 FTR Pro50	12h/12h	15°C (15d) → 6°C /11°C (3d)	proline-augmented
C. costata	LD	16h/8h	18°C (3w)	standard
	LD Pro50	16h/8h	18°C (5w)	proline-augmented
	SD	12h/12h	18°C (6w)	standard
	SDA	12h/12h → 0/24h*	18°C (6w) → 11°C (1w) → 4°C (4w)	standard

*, larvae were shifted to constant darkness on the day of their transfer to 11°C;

**, d, days; w, weeks; see text for more details.

Table S1. Summary of literature data on maximum ice fraction in various invertebrates.

Species and taxonomic affiliation	Geographic origin and acclimation status	IF_{max}* (% TBW)	Reference
Insecta			
Eleodes blanchardi (Coleoptera)	Norway, field-collected, overwintering adult	75	Zachariassen et al., 1979
Eurosta solidaginis (Diptera)	Ohio, New York, field-collected, overwintering larva	64	Lee and Lewis, 1985
Hemideina maori (Orthoptera)	New Zealand, field-collected, cold acclimated	82	Ramlov and Westh, 1993
Melasoma collaris (Coleoptera)	Norway, field-collected, cold acclimated	77	Gehrken and Southon, 1997
	ibid., warm-acclimated in lab.	84.5	
Celatoblatta quinquemaculata (Blattodea)	New Zealand, field-collected, overwintering adult	74	Block et al., 1998
Heleomyza borealis (Diptera)	Arctics, field-collected, overwintering larva	81	Worland et al., 2000
Tardigrada			
Adorybiotus coronifer	Greenland, field-collected in winter	79	Westh and Kristensen, 1992
	Greenland , field-collected in summer	89	
	ibid., cold-acclimated in lab.	83	
Amphibolus nebulosus	Greenland, field-collected in summer	88	
Halobiotus crispae	Denmark, field collected, active stage	69	Halberg et al., 2009
	ibid., diapause P1 stage	59	
Macrobiotus sapiens	Croatia, lab culture, active, starved	84.5	Hengherr et al., 2009
	ibid., cold-acclimated	81.1	
Paramacrobiotus richtersi	Germany, lab culture, active, starved	85.7	
	ibid., cold-acclimated	82.5	
Macrobiotus tonollii	Oregon, lab culture, active, starved	86.4	
	ibid., cold-acclimated	81.2	
Milnesium tardigradum	Germany, lab culture, active, starved	85.1	
	ibid., cold-acclimated	80.5	
Echinscus granulatus	Germany, field-collected, active, fed	83.8	
	ibid., cold-acclimated	78.0	
Echinscus testudo	Germany, field-collected, active, fed	84.3	
	ibid., cold-acclimated	80.5	
Nematoda			
Panagrolaimus davidi	Antarctics, lab culture, warm-acclimated,	82	Wharton and Block, 1997
Anelida			
Buchholzia apendiculata	Austria, field-collected, spring active	18.1	Block and Bauer, 2000
Buchholzia simplex		60.1	
Enchytraeus buchholzi		17.0	
Enchytraeus albidus		64.3	
Henlea ventriculosa		40.1	
Fridericia tubulosa		65.6	
Enchytraeus albidus	Germany, lab culture, acclimated to 5°C	61.4	Patricio Silva et al., 2013
	Greenland, lab culture, acclimated to 5°C	58.8	

* The IF_{max} was measured by gradual layer calorimetry (Zachariassen et al., 1979), or by a custom-made calorimeter registering heat absorbed during melting of frozen sample (Lee and Lewis, 1985), or by differental scanning calorimetry (DSC, most other studies). The ^{1}H nuclear magnetic resonance was used to determine the amount of unfrozen water in one study (Gehrken and Southon, 1997).

Table S2. Optimization of cryopreservation protocol for *Chymomyza costata* larvae.

Assay	Parameter value	n (replicates)	Survival (%)		
			larvae	puparia	adults
Control 1:	manipulation only	233 (4)	100	92,0	85,6
Control 2:	freezing only: -30°C / 1h	100 (2)	100	87,0	76,0
Cryopreservation protocols with variable values of assessed parameters:					
Rate r_1	1,5°C / min	80 (1)	55,0	0	0
	1°C /min	60 (1)	35,0	0	0
	0,5°C / min	60 (1)	73,4	13,3	6,7
	0,25°C / min	60 (1)	76,7	13,3	11,7
	0,17°C / min	60 (1)	95,0	28,3	23,3
	0,10°C / min	440 (7)	96,8	53,6	39,3
	0,05°C / min	60 (1)	83,3	28,3	13,3
Rate r_2	2 - 4°C / sec	440 (7)	96,8	53,6	39,3
	10 - 20°C / sec*	50 (1)	56,0	22,0	10,0
	20 - 60°C / sec**	20 (1)	45,0	0	0
Rate r_3	not assessed, maintained invariably between 1 - 2°C / sec				
Rate r_4	0,1°C /min	300 (3)	97,4	55,7	39,8
	0,2°C / min	60 (1)	98,4	43,3	30,0
	0,6°C / min	440 (7)	96,8	53,6	39,3
	1,2°C / min	60 (1)	92,4	15,0	0
Temperature T_1	-5°C	60 (1)	0	0	0
	-5°C*	30 (1)	0	0	0
	-10°C	60 (1)	0	0	0
	-15°C	80 (1)	0	0	0
	-20°C	269 (4)	16,3	0	0
	-22°C	120 (2)	68,4	7,5	5,9
	-24°C	220 (3)	79,5	10,6	7,8
	-26°C	220 (3)	92,6	13,4	8,9
	-28°C	120 (2)	98,4	10,0	5,9
	-30°C	440 (7)	96,8	53,6	39,3
	-35°C	160 (2)	100,0	45,7	28,2
	-40°C	340 (4)	98,1	23,7	15,2
Temperature T_2	-30°C	440 (7)	96,8	53,6	39,3
	-20°C	60 (1)	100,0	31,7	23,3
	-10°C	280 (3)	95,4	63,8	39,9
	-5°C	60 (1)	96,7	5,0	1,7
	0°C	60 (1)	78,3	0	0
	r.t.	40 (1)	65,0	0	0
Storage of *C. costata* larvae in LN_2 (cryopreserved using the optimal protocol) for various periods of time:					
Assay	Storage time	n (replicates)	larvae	puparia	adults
Optimal protocol	1 hour	440 (7)	96,8	53,6	39,3
	2 months	40 (1)	97,5	57,5	42,5
	4 months	80 (1)	95,0	22,5	10,0
	6 months	40 (1)	97,5	55,0	42,5
	9 months	180 (1)	97,2	20,6	13,3
	18 months	160 (1)	92,5	13,8	5,6

n, total number of larvae assessed. Number of biological replicates is shown in parentheses**.** Generally, variation in adult survival was relatively high not only between generations (biological replicates) abut also between replicated tubes of the same generation (technical replicates). For instance, the optimal protocol assay was replicated in (7) different generations with the following results (mean±S.D., range): larvae, 96.8±1.9, 93.3-98.8; puparia, 53.5±12.3, 41.7-70.0; adults, 39.4±13.5, 11.7-58.3. Because most other treatments were replicated only once or few times, we show final survival as a percentage of survivors from all individuals (generations pooled).

***,** larvae placed into copper capillary (5 cm long, 1.2 mm inner diameter, filled with distilled water), plunged to LN_2

****,** larvae placed into copper capillary, plunged to liquid propane held at -196°C

All parameters were assessed one by one. The values of the assessed parameter varied as shown in the Table (left column), while all other parameters were kept optimal. The optimal protocol is highlighted in blue.

Table S3. Metabolomic profiles in *Chymomyza costata* larvae of four acclimation variants.

	LD		SD		SDA		LD Pro50	
3-Alanine	1,19	0,00	t		t		t	
Alanine	6,69	0,54	6,98	0,48	3,42	0,12	4,26	0,67
Arginine	6,68	0,75	6,43	0,14	7,84	0,62	6,19	0,81
Asparagine	4,91	0,24	20,92	1,97	17,38	1,70	15,52	1,15
Aspartate	0,27	0,03	0,24	0,01	t		0,71	0,10
Cysteine	0,34	0,05	t		t		t	
Glutamine	19,43	1,24	120,61	10,05	24,96	5,12	153,89	57,83
Glutamate	8,63	0,47	5,47	0,35	6,26	0,26	7,55	0,76
Glycine	1,69	0,17	0,60	0,10	1,35	0,09	0,49	0,07
Histidine	7,23	0,79	1,53	0,23	2,07	0,32	t	
Isoleucine	1,10	0,18	0,64	0,03	0,59	0,05	0,74	0,04
Leucine	1,21	0,17	0,76	0,08	0,67	0,06	0,76	0,06
Lysine	1,72	0,30	3,50	0,46	1,57	0,14	1,06	0,24
Methionine	0,36	0,05	t		t		t	
Phenylalanine	0,88	0,02	0,57	0,05	0,63	0,04	0,75	0,08
Proline	31,41	2,11	161,75	12,75	339,08	19,31	487,02	22,95
Serine	1,91	0,25	2,12	0,31	1,48	0,15	1,22	0,19
Threonine	3,31	0,48	0,62	0,13	0,64	0,05	1,17	0,15
Trytophan	0,62	0,07	1,32	0,16	0,72	0,06	0,52	0,08
Tyrosine	5,55	0,93	3,17	0,04	2,58	0,20	2,11	0,37
Valine	2,18	0,26	1,01	0,04	0,84	0,13	1,08	0,23
Ornithine	0,26	0,02	0,31	0,06	t		t	
Sarcosine	0,34	0,03	0,25	0,05	0,38	0,04	0,00	0,00
Citrate	3,87	0,36	6,96	0,29	4,46	0,50	6,31	1,16
Ketoglutarate	t		0,73	0,14	t		t	
Malate	2,17	0,19	1,60	0,06	0,99	0,11	2,51	0,16
Succinate	1,23	0,35	t		t		t	
Lactate	2,95	0,18	2,29	2,24	0,58	0,10	t	
Glycerol	0,19	0,01	0,16	0,02	0,23	0,04	0,32	0,13
Erythritol	0,04	0,00	0,14	0,01	0,18	0,04	0,29	0,08
Mannitol	t		0,05	0,01	0,04	0,00	0,18	0,08
Sorbitol	t		0,47	0,04	0,60	0,03	2,28	0,81
chiro-Inositol	0,21	0,02	0,16	0,01	0,30	0,02	0,23	0,05
myo-Inositol	0,13	0,01	0,09	0,01	0,12	0,01	0,22	0,02
Fructose	0,37	0,02	0,68	0,02	0,77	0,08	1,43	0,37
Glucose	2,05	0,32	0,40	0,06	0,37	0,04	0,61	0,10
Trehalose	23,54	3,25	22,87	1,31	52,36	3,61	50,55	1,01
Total	143,62	9,76	374,29	27,73	473,48	24,85	749,98	80,54

Each value represents mean ± S.D. of four biological replicates (each consisting of a pool of 5 larvae).
All data are expressed as mmol.kg^{-1} TBW. Three most abundant metabolites are highlighted in yellow fields.
t, traces of metabolite present (below the threshold for reliable quantitation).

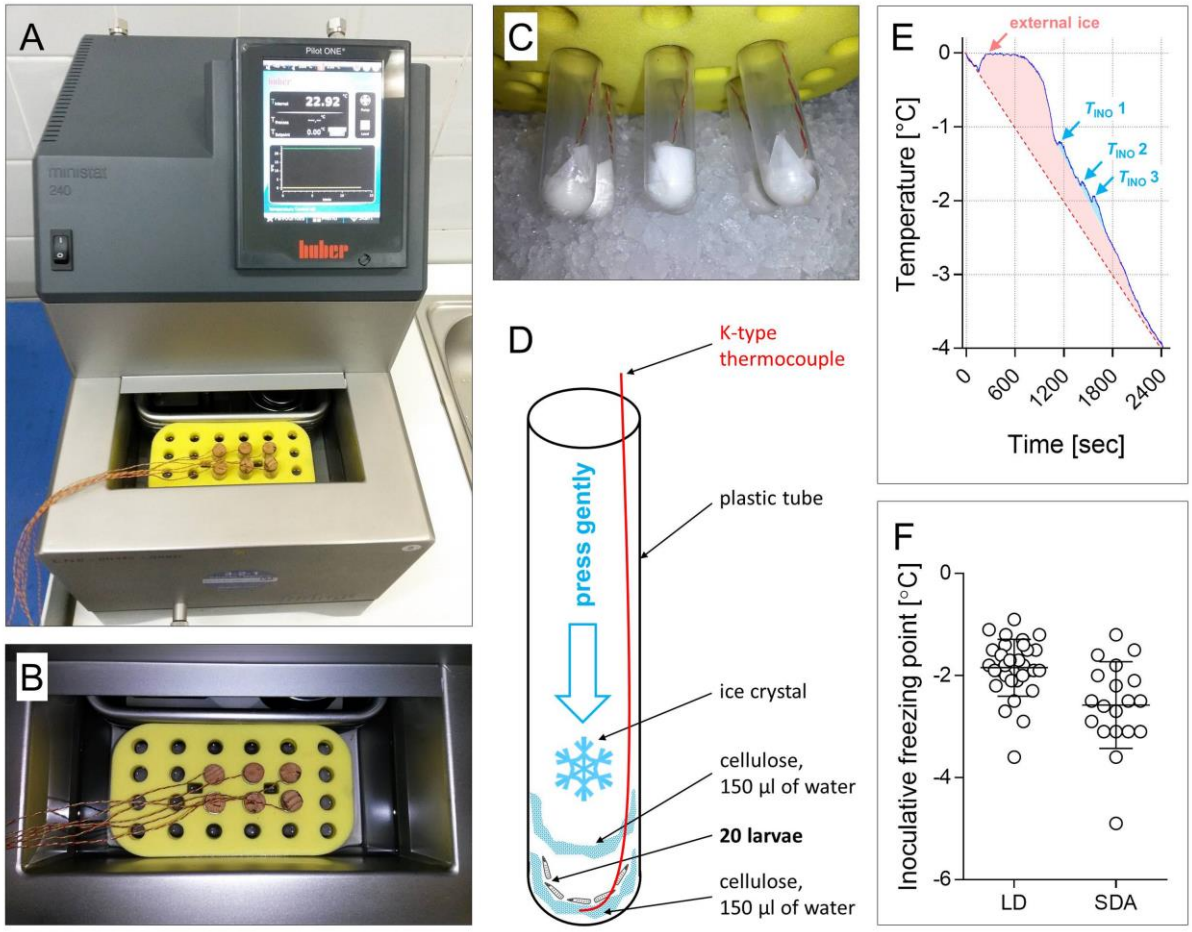

Fig. S1. Ice nucleation of larval body fluids with external ice crystals in Ministat 240 cooling circulator, Huber.

(A-C) Photographs show placement of six plastic test tubes (1 cm in diam., 5 cm long), each containing different number of larvae (5 – 20) depending on experiment, inside the Huber Ministat. The tubes were inserted into holes of a floating island and submerged to cooling medium (Thermofluid SilOil, M60 115/200.05, Huber). (D) Schematic view of the arrangements inside each plastic test tube. Larvae were placed on a small piece of cellulose (75 mg) that was moistened with 150 uL of distilled water. Similar piece of moistened cellulose was placed over the larvae and slightly pressed, which ensured that all larvae were in a tight contact with moisture. The thermocouple was mounted in between the two pieces of cellulose. A small ice crystal was added on top of wet cellulose, the tube was closed using cork plug and temperature program was started in Huber Ministat. (E) An example of temperature record (PicoLog TC-08 datalogger) in an experiment where five larvae of *Chymomyza costata* (acclimation variant LD) were slowly cooled (cooling rate 0.1ºC min^{-1}) in the tube arranged as described on D). Large freeze exotherm (red area) belongs to external water in cellulose. Three small freeze exotherms (blue areas) were detected, which belong to three larvae seeded by external ice crystals. (F) Results of replicated experiments as described in E). The *Chymomyza costata* larvae of two acclimation variants were measured: LD (n = 40), SDA (n = 25) (see Table 1 for detailed description of acclimation variants). All recorded larval freeze exotherms (inoculation freezing points, T_{INO}) are shown: LD (n = 31; mean = -1.85; S.D. = 0.56), SDA (n = 19; mean = -2.58; S.D. = 0.85), the means of LD and SDA group are statistically different (t-test, t = 3.680, P = 0.0006).

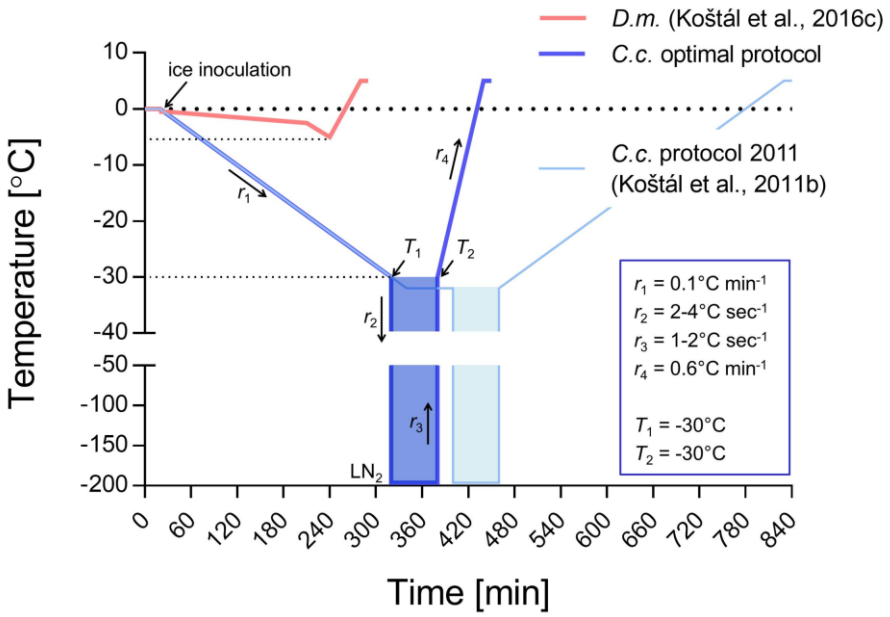

Fig. S2. Freezing and cryopreservation protocols.

In all protocols, larval freezing was initiated by contact with external ice crystals (ice inoculation) at relatively high sub-zero temperatures (see Fig. S1). The protocol used for larvae of *Drosophila melanogaster* (*D.m.*, red line) was previously optimized and published in Koštál et al. (2016c). The protocol used previously for cryopreservation of larvae of *Chymomyza costata* (*C.c.*, pale blue line, Koštál et al., 2011b) was further optimized in this study (Table S1) and the optimum parameters (ensuring the highest survival of adults) are listed in the blue frame and shown graphically as dark blue line (the rates of cooling/heating are shown as r_1, r_2, r_3 and r_4. At temperature T_1, frozen larvae are plunged into liquid nitrogen (LN_2), and, later, returned to Huber Ministat pre-set to T_2 temperature).

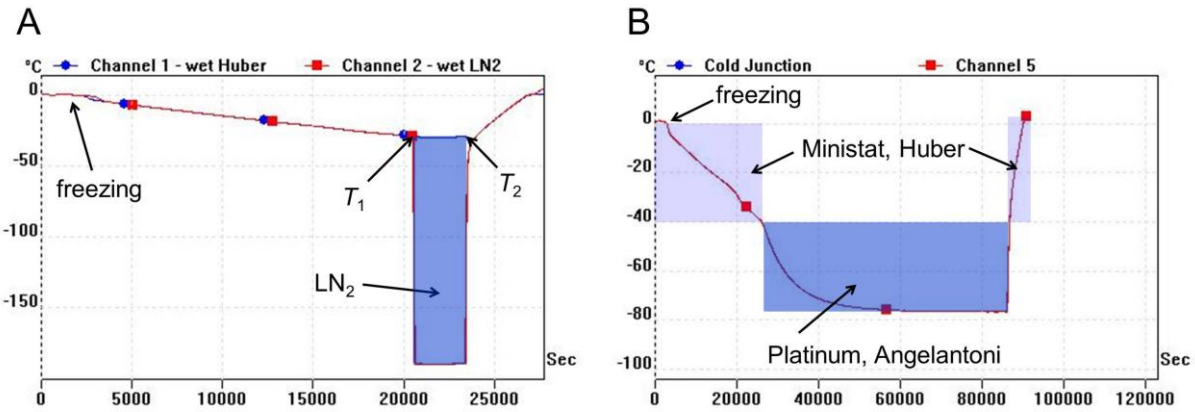

Fig. S3. Examples of temperature record from PicoLog TC-08 datalogger.

(A) Freezing to -30°C / 1h (Channel 1, blue line) and freezing to a T_1 = -30°C followed by 1h in liquid nitrogen (LN_2, Channel 2, red line). Note that both channels show freeze exotherms (water in the cellulose wrapping) extending over approximately 1st hour of slow cooling (rate 0.1°C min^{-1}). External ice crystals inoculate larvae inside the wrapping (see Fig. S1 E). (B) Slow freezing to -40°C in Ministat (Huber) followed by transfer to Platinum freezer (Angelantoni), where the sample gradually cooled to -75°C (Channel 5, red line).

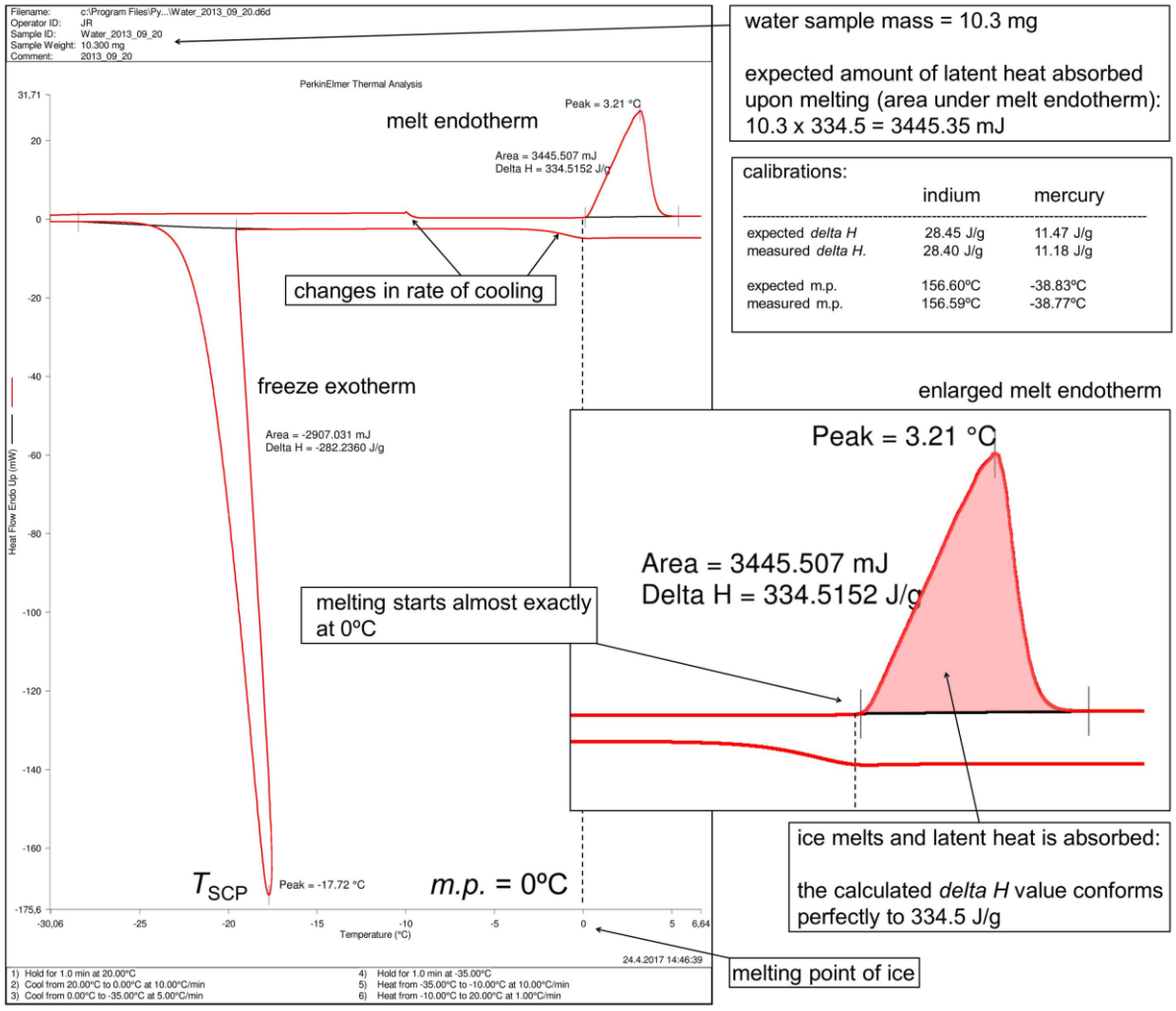

Fig. S4. DSC calibration: example protocol (distilled water).

The temperature scale and the heat flow of DSC4000 instrument were calibrated using indium, mercury and distilled water standards. Calibration parameters for indium and mercury are shown in the frame (right). An example protocol (left) shows that running the thermal analysis of distilled water sample (10.3 mg) returns expected values of melting point (m.p., 0ºC) and specific enthalpy of ice/water transition (*delta H*, 334.5 J g^{-1}) (Wang and Weller, 2011).

Wang, L., Weller, C.L. (2011) Thermophysical properties of frozen foods. In *Handbook of Frozen Food Processing and Packaging*, 2nd edition (ed. D.-W. Sun), pp. 101-125. Boca Raton: CRC Press.

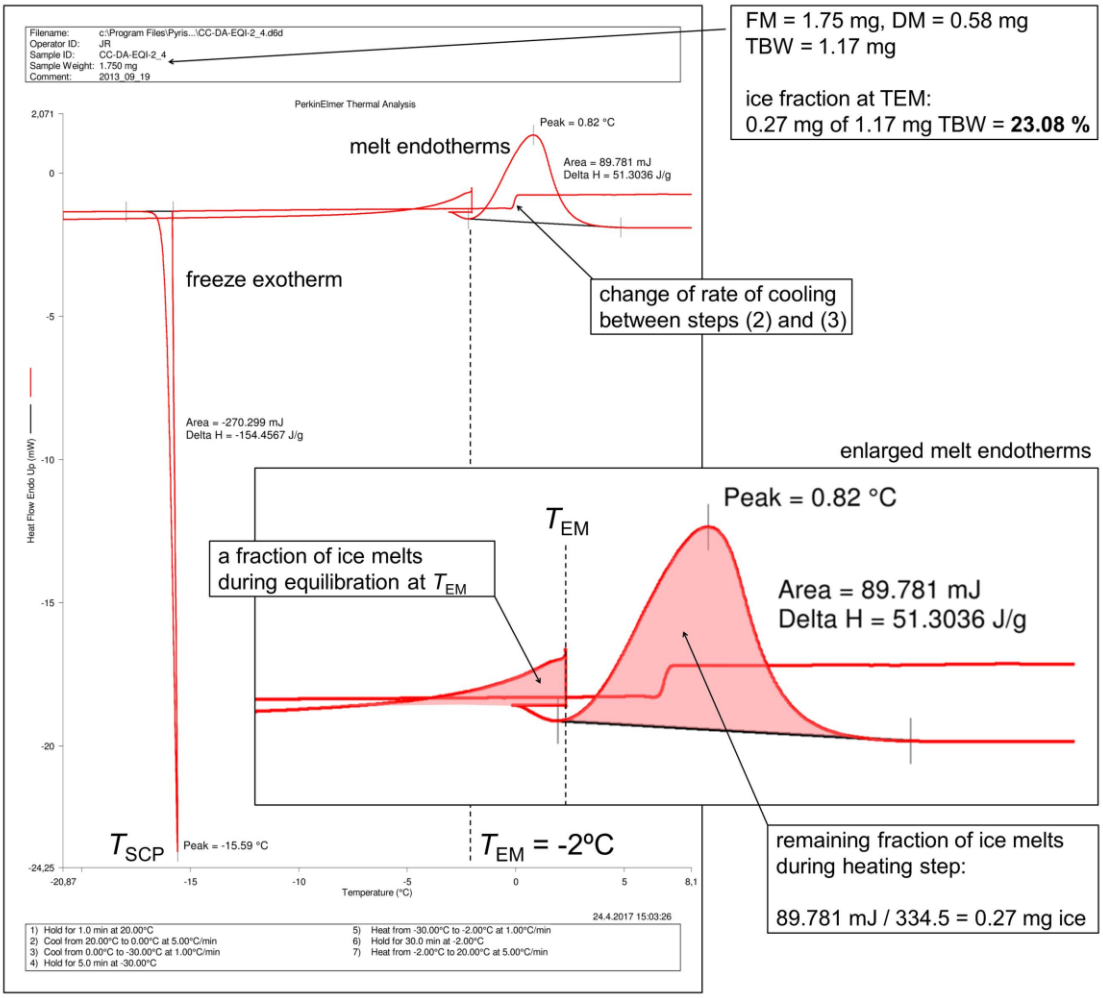

Fig. S5. *Equi-melt* thermal analysis: example protocol (*C. costata*, SDA).

The *Equi-melt* temperature programme: (1) hold for 1 min at 20ºC; (2) cool to 0ºC at a rate 5ºC min^{-1}; (3) cool to -30ºC at a rate 1ºC min^{-1}; (4) hold for 5 min at -30ºC; (5) heat to *Equi-melt* temperature (T_{EM}) at a rate 1ºC min^{-1}; (6) hold for 30 min at T_{EM}; (7) heat to 20ºC at a rate 5ºC min^{-1}.

Notes:

steps (3 and 4): the temperature of -30ºC was sufficient to reach maximum ice fraction in all treatments. We verified in preliminary experiments that neither exposing the larvae to lower temperature (down to -70ºC), nor extending the time of exposure at -30ºC (up to 48 hours) did further increase the ice fraction;

steps (5 and 6): the ice fraction equilibrates to specific T_{EM} that varied from -30ºC to -0.5ºC (in addition, T_{EM} of -50ºC was analyzed for *C. costata* SDA variant, see Fig. S7 C);

step (7): the ice fraction was calculated from the area under melt endotherm using the value of *delta H* = 334.5 J g^{-1} as the enthalpy of ice/water transition.

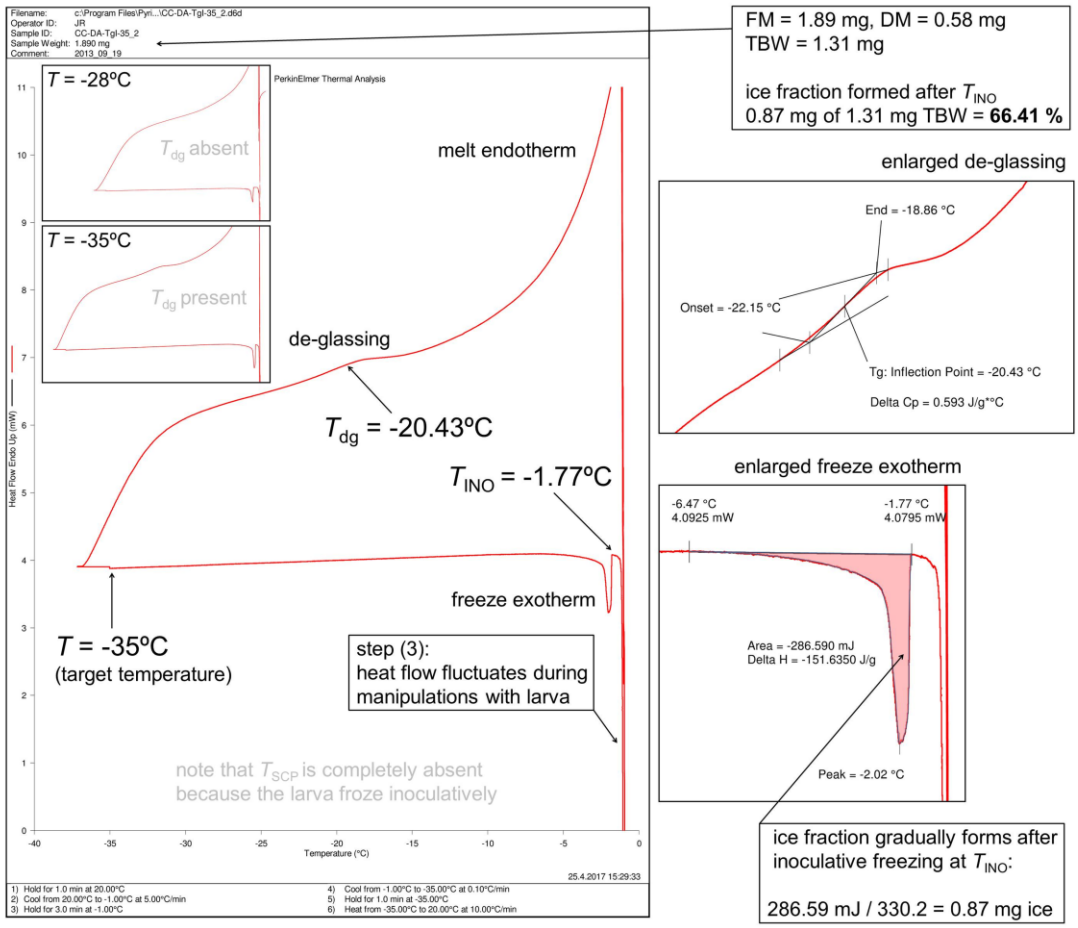

Fig. S6. *Ino-freeze* thermal analysis: example protocol (*C. costata*, SDA).

The *Ino-freeze* temperature programme: (1) hold for 1 min at 20°C; (2) cool to -1°C at a rate 5°C min^{-1}; (3) hold for 3 min -1°C and, meanwhile, open the instrument and insert aluminum pan bottom lined with filter paper disc (SS-033, Wescor) to which 10 uL of distilled water was applied and then submerged in liquid nitrogen to freeze it. Next, after the bottom of test-pan equilibrates to programmed temperature of -1°C (approximately within 10 sec), add larva, cover the bottom loosely with lid and close the instrument; (4) cool to target temperature at a rate 0.1°C min^{-1}; (5) hold for 1 min at target temperature; (6) heat to 20°C at a fast rate 10°C min^{-1}.

Notes:

steps (1 and 2): performed with the reference pan only inside instrument;

step (3): the test pan and larva were added. When performed carefully, this critical step ensures that all larvae are exposed to external ice crystals at exactly -1°C;

steps (4 and 5): the target temperature can be varied in order to see whether or not the de-glassing transition (T_{dg}) occurs upon rapid heating back to 20°C [when it occurs, it indicates that the vitrification transition (T_g) must have occurred during previous slow cooling to target temperature. Otherwise, glass trasition is not observable by DSC method at slow cooling rates]. However, observing only the specific aim of inoculative ice fraction analysis, the target temperature of -10°C would be sufficient as all larval freeze exotherms ended between -3°C and -5°C (see data in Fig. S11). The ice fraction was calculated from freeze exotherms and the enthalpy of water/ice transition (*delta H*) was modified according to the exact peak temperature of inoculative freezing (T_{INO} = -2.02°C in this example) using the formula:

$delta\ H = 334.5 + 2.12\ T_{INO} + 0.0042\ (T_{INO})^2 = 330.2$ (Wang and Weller, 2011)

step (6): the fast rate of heating (10°C min^{-1}) facilitates the observation of de-glassing (T_{dg}) transition.

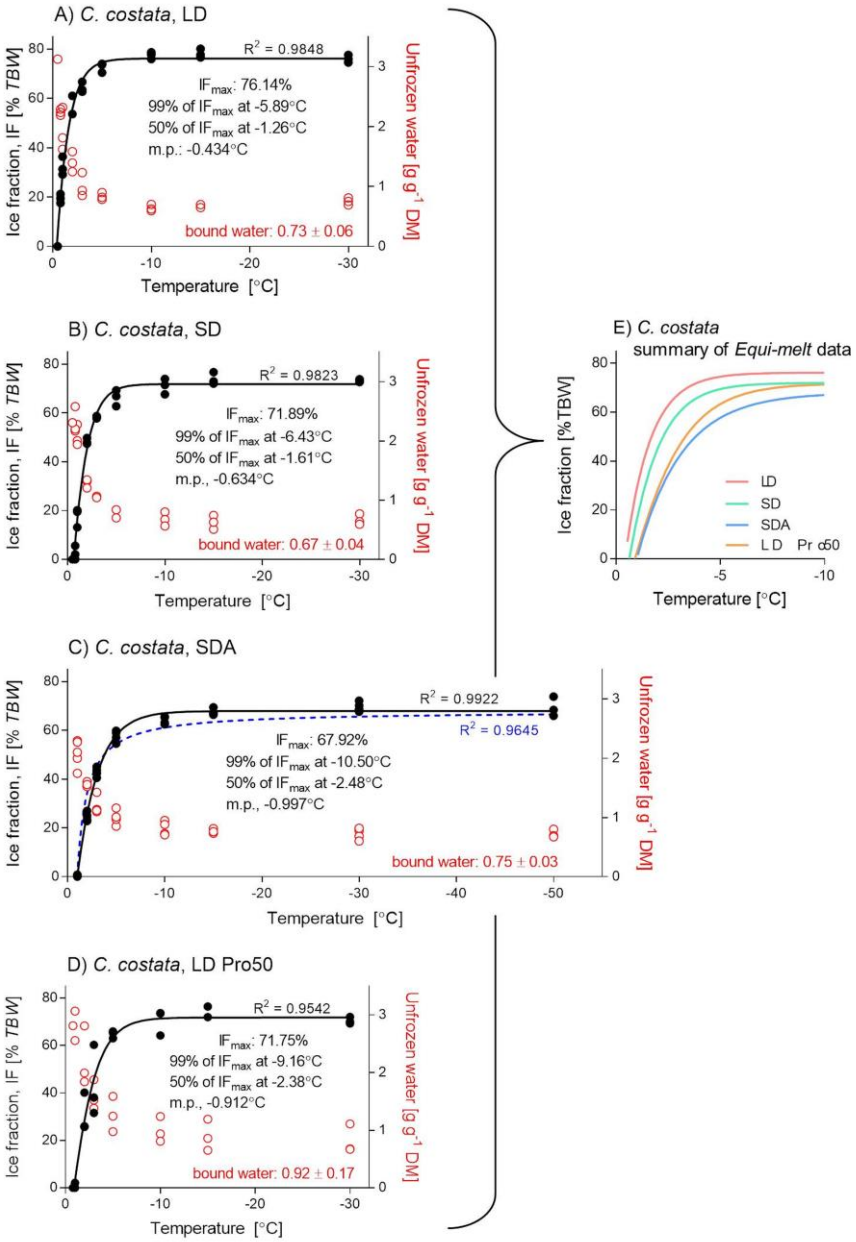

Fig. S7. Summary of *Equi-melt* data for *Chymomyza costata*

The *Equi-melt* thermal analyses were run with different target temperatures (*T*) ranging between -0.5°C and -30°C (or -50°C in SDA variant). At least three larvae were analyzed for each experimental variant (A-D) and target temperature combination (three data-points). The Boltzmann sigmoids were fitted to empirical data (black solid lines). For comparison, an example of a theoretical freezing curve (dashed blue line) *vs.* Boltzmann sigmoid fitting is shown in (C):

theoretical freezing curve (Wang and Weller., 2011): $IF = OAW*(1 - (m.p./T)$

Boltzmann sigmoid: $IF = OAW + (top – OAW)/(1 + \exp((V50-x)/slope))$

All other parameters (IF_{max}; 99% of IF_{max}; 50% of IF_{max}; m.p.) were derived from Boltzmann sigmoids. The amount of unfrozen water per mg DM for each larva is shown as red circle. Bound water (OIW) is calculated as a bottom of a Boltzmann sigmoid fitted to unfrozen water data.

(E) A summary figure showing only the *Equi-melt* curves for each treatment (these lines are used in Fig. 2A).

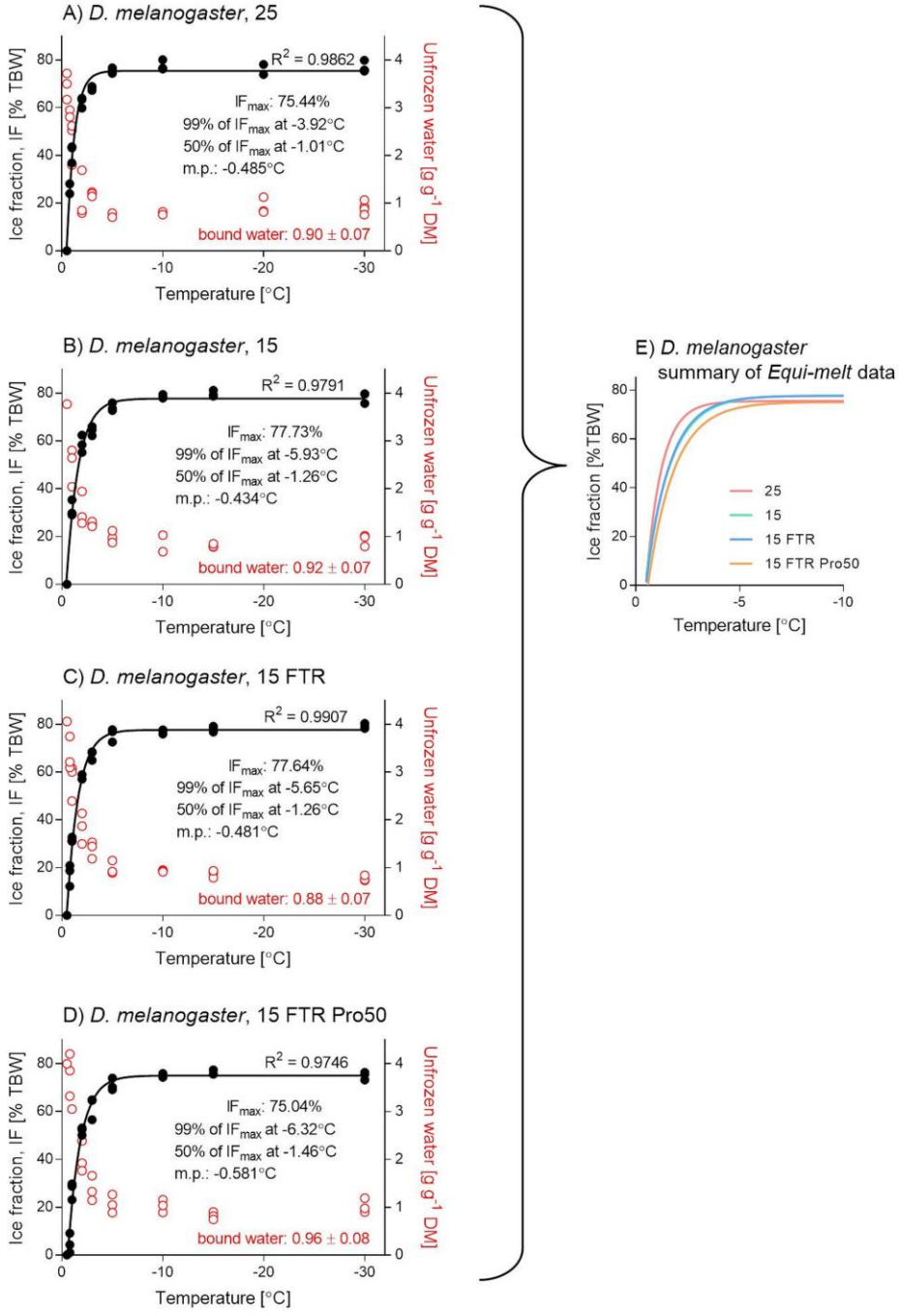

Fig. S8. Summary of *Equi-melt* data for *Drosophila melanogaster*.

All descriptions as in Fig. S7**.**
(E) A summary figure showing only the *Equi-melt* curves for each treatment (these lines are used in Fig. 2E).

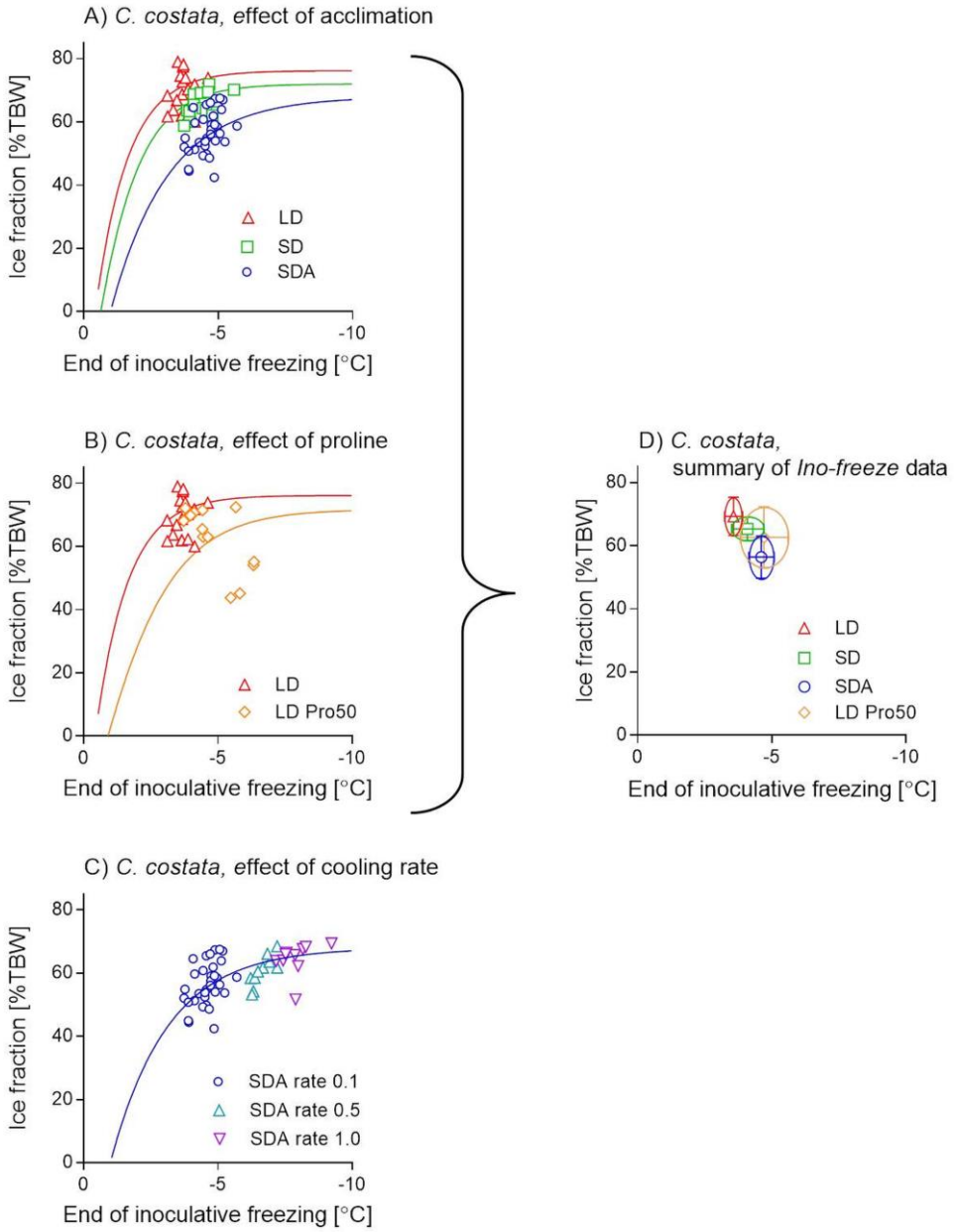

Fig. S9. Summary of *Ino-freeze* data for *Chymomyza costata.*

The *Ino-freeze* thermal analyses were run for individual larvae (points). Detailed results of *Ino-freeze* analyses are summarised in Fig. S11. *Equi-melt* curves (taken from Fig. S7) are also shown in order to allow direct comparison of the ice fraction analyzed by two methods. Note that *Ino-freeze* points and *Equi-melt* lines match very well. (A) Three acclimation variants (treatments LD, SD, SDA). (B) The effect of proline augmented diet (LD *vs.* LD Pro50). (C) The effect of cooling rate during the step (ii.) of freezing protocol. Three different cooling rates were compared: 0.1°C min^{-1}; 0.5°C min^{-1}; 1°C min^{-1}. The points express the ice fraction calculated from area under inoculative freeze exotherm at a temperature corresponding to the end of inoculative freezing (see Fig. S6).
(D) A summary figure showing ellipses based on mean x ± S.D. and mean y ± S.D. values of all *Ino-freeze* data points for each treatment (these ellipses are used in Fig. 2A).

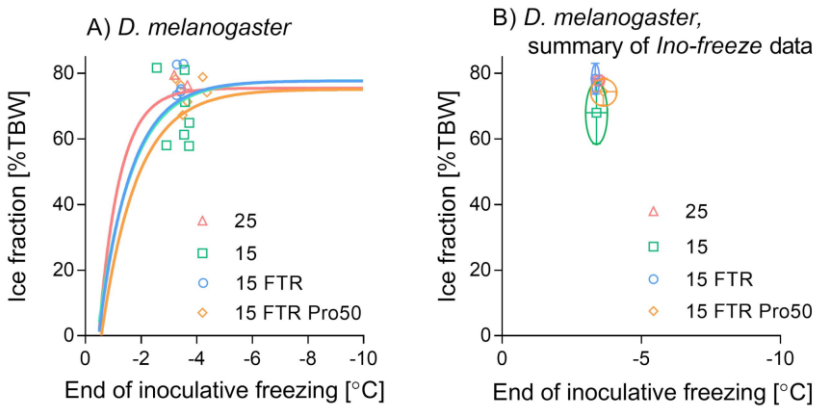

Fig. S10. Summary all *Ino-freeze* data for *Drosophila melanogaster*

All descriptions as in Fig. S9**.**
(B) A summary figure showing ellipses based on mean x ± S.D. and mean y ± S.D. values of all *Ino-freeze* data points for each treatment (these ellipses are used in Fig. 2E).

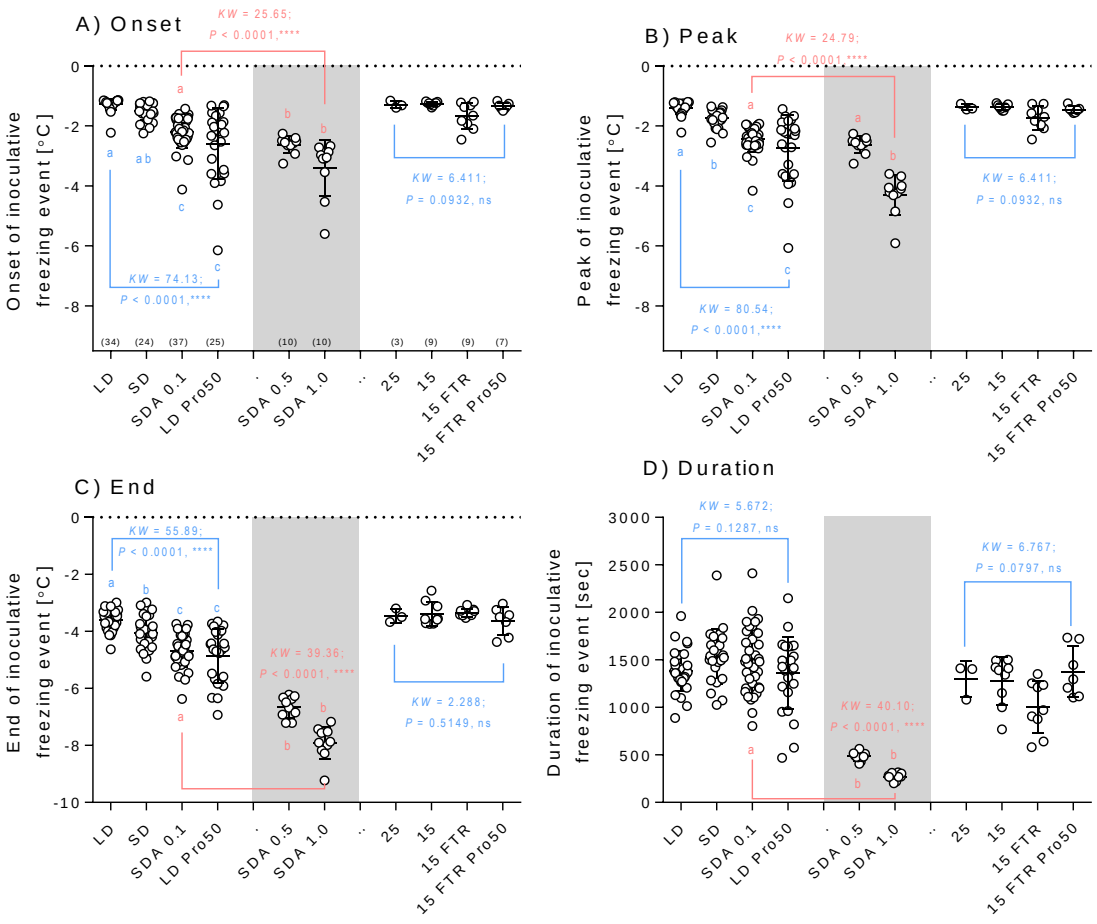

Figure S11. Summary of data obtained by *Ino-freeze* thermal analyses.

The parameters of inoculative freezing event [onset (= T_{INO}), peak, end, and duration; see Fig. S6 for more explanations] in variously treated larvae of *C. costata* (LD, SD, SDA, LD Pro50) and *D. melanogaster* (25, 15, 15 FTR, 15 FTR Pro50). In addition, the effect of cooling rate during the step (ii.) of freezing protocol was analyzed in *C. costata*. Three different cooling rates were compared: 0.1°C min^{-1}; 0.5°C min^{-1}; 1°C min^{-1}. Each point represents single thermal analysis (single larva). Number of larvae analyzed in each treatment (n) is shown in parentheses in (A). Note that there is a good match between the data on onset of inoculative freezing analyzed by DSC (Fig. S11 A) and similar data recorded directly by thermocouples in freeze-tolerance assays (Fig. S1 F). The differences between treatments (shown by blue and red lines) were assessed using Kruskal-Wallis nonparametric test (*KW* statistics is shown) followed by Dunn's multiple comparison test. Treatments flanked by different letter were statistically different according to the Dunn's test.

Table S1. Summary of literature data on maximum ice fraction in various invertebrates.

Species and taxonomic affiliation	Geographic origin and acclimation status	IF_{max} * (% TBW)	Reference
Insecta			
Eleodes blanchardi (Coleoptera)	Norway, field-collected, overwintering adult	75	Zachariassen et al., 1979
Eurosta solidaginis (Diptera)	Ohio, New York, field-collected, overwintering larva	64	Lee and Lewis, 1985
Hemideina maori (Orthoptera)	New Zealand, field-collected, cold acclimated	82	Ramlov and Westh, 1993
Melasoma collaris (Coleoptera)	Norway, field-collected, cold acclimated	77	Gehrken and Southon, 1997
	ibid., warm-acclimated in lab.	84.5	
Celatoblatta quinquemaculata (Blattodea)	New Zealand, field-collected, overwintering adult	74	Block et al., 1998
Heleomyza borealis (Diptera)	Arctics, field-collected, overwintering larva	81	Worland et al., 2000
Tardigrada			
Adorybiotus coronifer	Greenland, field-collected in winter	79	Westh and Kristensen, 1992
	Greenland, field-collected in summer	89	
	ibid., cold-acclimated in lab.	83	
Amphibolus nebulosus	Greenland, field-collected in summer	88	
Halobiotus crispae	Denmark, field collected, active stage	69	Halberg et al., 2009
	ibid., diapause P1 stage	59	
Macrobiotus sapiens	Croatia, lab culture, active, starved	84.5	Hengherr et al., 2009
	ibid., cold-acclimated	81.1	
Paramacrobiotus richtersi	Germany, lab culture, active, starved	85.7	
	ibid., cold-acclimated	82.5	
Macrobiotus tonollii	Oregon, lab culture, active, starved	86.4	
	ibid., cold-acclimated	81.2	
Milnesium tardigradum	Germany, lab culture, active, starved	85.1	
	ibid., cold-acclimated	80.5	
Echinscus granulatus	Germany, field-collected, active, fed	83.8	
	ibid., cold-acclimated	78.0	
Echinscus testudo	Germany, field-collected, active, fed	84.3	
	ibid., cold-acclimated	80.5	
Nematoda			
Panagrolaimus davidi	Antarctics, lab culture, warm-acclimated,	82	Wharton and Block, 1997
Anelida			
Buchholzia apendiculata	Austria, field-collected, spring active	18.1	Block and Bauer, 2000
Buchholzia simplex		60.1	
Enchytraeus buchholzi		17.0	
Enchytraeus albidus		64.3	
Henlea ventriculosa		40.1	
Fridericia tubulosa		65.6	
Enchytraeus albidus	Germany, lab culture, acclimated to 5°C	61.4	Patricio Silva et al., 2013
	Greenland, lab culture, acclimated to 5°C	58.8	

* The IF_{max} was measured by gradual layer calorimetry (Zachariassen et al., 1979), or by a custom-made calorimeter registering heat absorbed during melting of frozen sample (Lee and Lewis, 1985), or by differental scanning calorimetry (DSC, most other studies). The ^{1}H nuclear magnetic resonance was used to determine the amount of unfrozen water in one study (Gehrken and Southon, 1997).

Table S2. Optimization of cryopreservation protocol for *Chymomyza costata* larvae.

Assay	Parameter value	n (replicates)	Survival (%)		
			larvae	puparia	adults
Control 1:	manipulation only	233 (4)	100	92,0	85,6
Control 2:	freezing only: -30°C / 1h	100 (2)	100	87,0	76,0
Cryopreservation protocols with variable values of assessed parameters:					
Rate r_1	1,5°C / min	80 (1)	55,0	0	0
	1°C /min	60 (1)	35,0	0	0
	0,5°C / min	60 (1)	73,4	13,3	6,7
	0,25°C / min	60 (1)	76,7	13,3	11,7
	0,17°C / min	60 (1)	95,0	28,3	23,3
	0,10°C / min	440 (7)	96,8	53,6	39,3
	0,05°C / min	60 (1)	83,3	28,3	13,3
Rate r_2	2 - 4°C / sec	440 (7)	96,8	53,6	39,3
	10 - 20°C / sec*	50 (1)	56,0	22,0	10,0
	20 - 60°C / sec**	20 (1)	45,0	0	0
Rate r_3	not assessed, maintained invariably between 1 - 2°C / sec				
Rate r_4	0,1°C /min	300 (3)	97,4	55,7	39,8
	0,2°C / min	60 (1)	98,4	43,3	30,0
	0,6°C / min	440 (7)	96,8	53,6	39,3
	1,2°C / min	60 (1)	92,4	15,0	0
Temperature T_1	-5°C	60 (1)	0	0	0
	-5°C*	30 (1)	0	0	0
	-10°C	60 (1)	0	0	0
	-15°C	80 (1)	0	0	0
	-20°C	269 (4)	16,3	0	0
	-22°C	120 (2)	68,4	7,5	5,9
	-24°C	220 (3)	79,5	10,6	7,8
	-26°C	220 (3)	92,6	13,4	8,9
	-28°C	120 (2)	98,4	10,0	5,9
	-30°C	440 (7)	96,8	53,6	39,3
	-35°C	160 (2)	100,0	45,7	28,2
	-40°C	340 (4)	98,1	23,7	15,2
Temperature T_2	-30°C	440 (7)	96,8	53,6	39,3
	-20°C	60 (1)	100,0	31,7	23,3
	-10°C	280 (3)	95,4	63,8	39,9
	-5°C	60 (1)	96,7	5,0	1,7
	0°C	60 (1)	78,3	0	0
	r.t.	40 (1)	65,0	0	0
Storage of *C. costata* larvae in LN_2 (cryopreserved using the optimal protocol) for various periods of time:					
Assay	Storage time	n (replicates)	larvae	puparia	adults
Optimal protocol	1 hour	440 (7)	96,8	53,6	39,3
	2 months	40 (1)	97,5	57,5	42,5
	4 months	80 (1)	95,0	22,5	10,0
	6 months	40 (1)	97,5	55,0	42,5
	9 months	180 (1)	97,2	20,6	13,3
	18 months	160 (1)	92,5	13,8	5,6

n, total number of larvae assessed. Number of biological replicates is shown in parentheses. Generally, variation in adult survival was relatively high not only between generations (biological replicates) abut also between replicated tubes of the same generation (technical replicates). For instance, the optimal protocol assay was replicated in (7) different generations with the following results (mean±S.D., range): larvae, 96.8±1.9, 93.3-98.8; puparia, 53.5±12.3, 41.7-70.0; adults, 39.4±13.5, 11.7-58.3. Because most other treatments were replicated only once or few times, we show final survival as a percentage of survivors from all individuals (generations pooled).

***,** larvae placed into copper capillary (5 cm long, 1.2 mm inner diameter, filled with distilled water), plunged to LN_2

****,** larvae placed into copper capillary, plunged to liquid propane held at -196°C

All parameters were assessed one by one. The values of the assessed parameter varied as shown in the Table (left column), while all other parameters were kept optimal. The optimal protocol is highlighted in blue.

Table S3. Metabolomic profiles in *Chymomyza costata* larvae of four acclimation variants.

	LD		SD		SDA		LD Pro50	
3-Alanine	1,19	0,00	t		t		t	
Alanine	6,69	0,54	6,98	0,48	3,42	0,12	4,26	0,67
Arginine	6,68	0,75	6,43	0,14	7,84	0,62	6,19	0,81
Asparagine	4,91	0,24	20,92	1,97	17,38	1,70	15,52	1,15
Aspartate	0,27	0,03	0,24	0,01	t		0,71	0,10
Cysteine	0,34	0,05	t		t		t	
Glutamine	19,43	1,24	120,61	10,05	24,96	5,12	153,89	57,83
Glutamate	8,63	0,47	5,47	0,35	6,26	0,26	7,55	0,76
Glycine	1,69	0,17	0,60	0,10	1,35	0,09	0,49	0,07
Histidine	7,23	0,79	1,53	0,23	2,07	0,32	t	
Isoleucine	1,10	0,18	0,64	0,03	0,59	0,05	0,74	0,04
Leucine	1,21	0,17	0,76	0,08	0,67	0,06	0,76	0,06
Lysine	1,72	0,30	3,50	0,46	1,57	0,14	1,06	0,24
Methionine	0,36	0,05	t		t		t	
Phenylalanine	0,88	0,02	0,57	0,05	0,63	0,04	0,75	0,08
Proline	31,41	2,11	161,75	12,75	339,08	19,31	487,02	22,95
Serine	1,91	0,25	2,12	0,31	1,48	0,15	1,22	0,19
Threonine	3,31	0,48	0,62	0,13	0,64	0,05	1,17	0,15
Trytophan	0,62	0,07	1,32	0,16	0,72	0,06	0,52	0,08
Tyrosine	5,55	0,93	3,17	0,04	2,58	0,20	2,11	0,37
Valine	2,18	0,26	1,01	0,04	0,84	0,13	1,08	0,23
Ornithine	0,26	0,02	0,31	0,06	t		t	
Sarcosine	0,34	0,03	0,25	0,05	0,38	0,04	0,00	0,00
Citrate	3,87	0,36	6,96	0,29	4,46	0,50	6,31	1,16
Ketoglutarate	t		0,73	0,14	t		t	
Malate	2,17	0,19	1,60	0,06	0,99	0,11	2,51	0,16
Succinate	1,23	0,35	t		t		t	
Lactate	2,95	0,18	2,29	2,24	0,58	0,10	t	
Glycerol	0,19	0,01	0,16	0,02	0,23	0,04	0,32	0,13
Erythritol	0,04	0,00	0,14	0,01	0,18	0,04	0,29	0,08
Mannitol	t		0,05	0,01	0,04	0,00	0,18	0,08
Sorbitol	t		0,47	0,04	0,60	0,03	2,28	0,81
chiro-Inositol	0,21	0,02	0,16	0,01	0,30	0,02	0,23	0,05
myo-Inositol	0,13	0,01	0,09	0,01	0,12	0,01	0,22	0,02
Fructose	0,37	0,02	0,68	0,02	0,77	0,08	1,43	0,37
Glucose	2,05	0,32	0,40	0,06	0,37	0,04	0,61	0,10
Trehalose	23,54	3,25	22,87	1,31	52,36	3,61	50,55	1,01
Total	143,62	9,76	374,29	27,73	473,48	24,85	749,98	80,54

Each value represents mean ± S.D. of four biological replicates (each consisting of a pool of 5 larvae).
All data are expressed as mmol.kg^{-1} TBW. Three most abundant metabolites are highlighted in yellow fields.
t, traces of metabolite present (below the threshold for reliable quantitation).

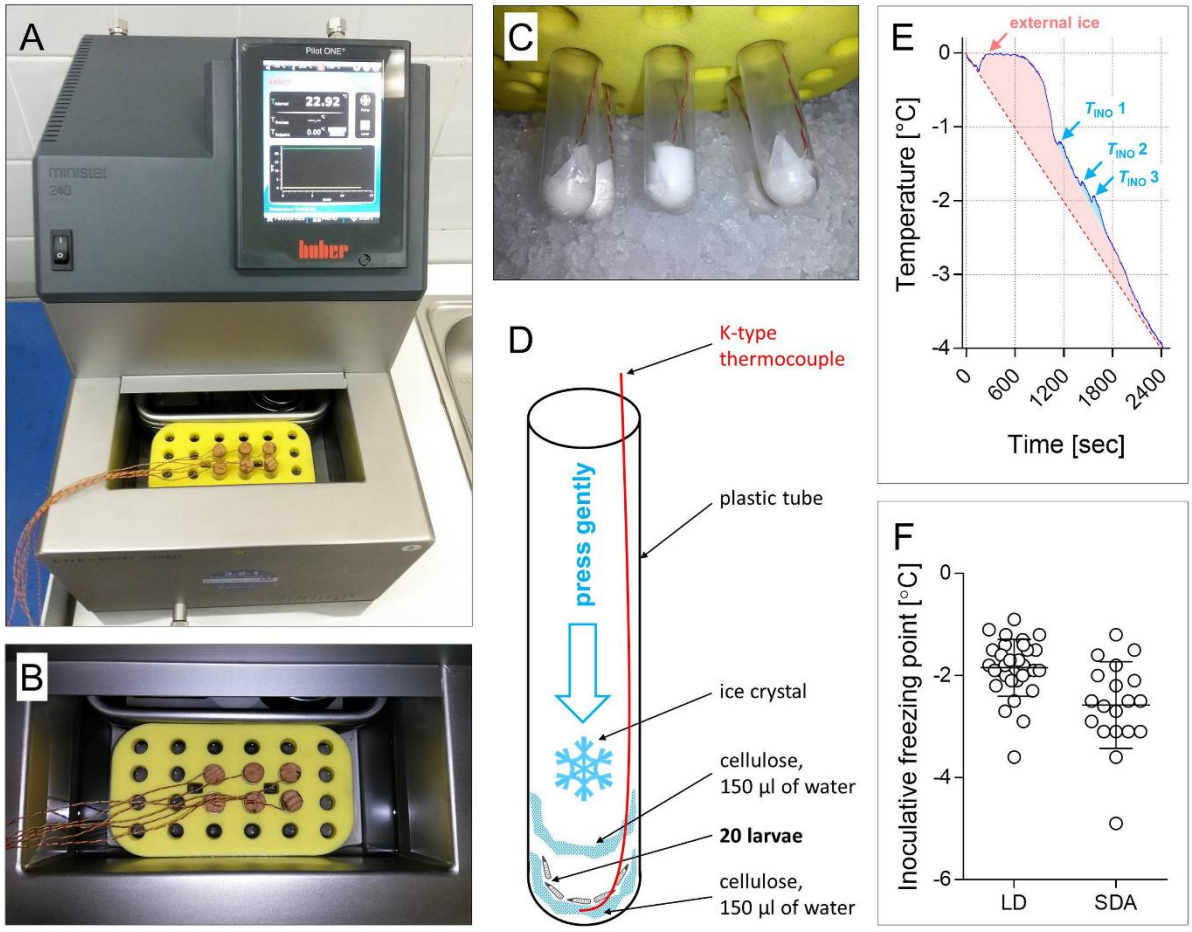

Fig. S1. Ice nucleation of larval body fluids with external ice crystals in Ministat 240 cooling circulator, Huber.

(A-C) Photographs show placement of six plastic test tubes (1 cm in diam., 5 cm long), each containing different number of larvae (5 – 20) depending on experiment, inside the Huber Ministat. The tubes were inserted into holes of a floating island and submerged to cooling medium (Thermofluid SilOil, M60 115/200.05, Huber). (D) Schematic view of the arrangements inside each plastic test tube. Larvae were placed on a small piece of cellulose (75 mg) that was moistened with 150 uL of distilled water. Similar piece of moistened cellulose was placed over the larvae and slightly pressed, which ensured that all larvae were in a tight contact with moisture. The thermocouple was mounted in between the two pieces of cellulose. A small ice crystal was added on top of wet cellulose, the tube was closed using cork plug and temperature program was started in Huber Ministat. (E) An example of temperature record (PicoLog TC-08 datalogger) in an experiment where five larvae of *Chymomyza costata* (acclimation variant LD) were slowly cooled (cooling rate 0.1ºC min^{-1}) in the tube arranged as described on D). Large freeze exotherm (red area) belongs to external water in cellulose. Three small freeze exotherms (blue areas) were detected, which belong to three larvae seeded by external ice crystals. (F) Results of replicated experiments as described in E). The *Chymomyza costata* larvae of two acclimation variants were measured: LD (n = 40), SDA (n = 25) (see Table 1 for detailed description of acclimation variants). All recorded larval freeze exotherms (inoculation freezing points, T_{INO}) are shown: LD (n = 31; mean = -1.85; S.D. = 0.56), SDA (n = 19; mean = -2.58; S.D. = 0.85), the means of LD and SDA group are statistically different (t-test, t = 3.680, P = 0.0006).

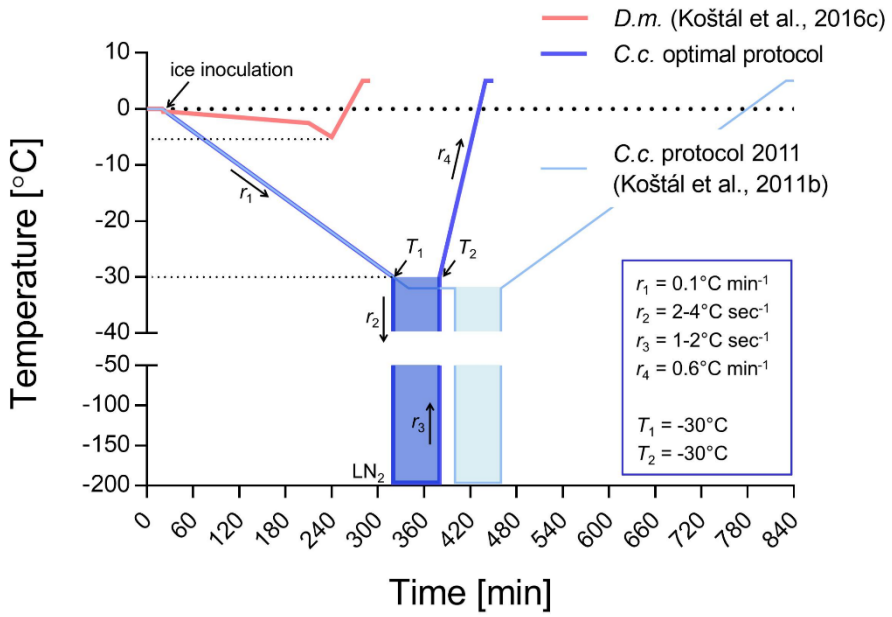

Fig. S2. Freezing and cryopreservation protocols.

In all protocols, larval freezing was initiated by contact with external ice crystals (ice inoculation) at relatively high sub-zero temperatures (see Fig. S1). The protocol used for larvae of *Drosophila melanogaster* (*D.m.*, red line) was previously optimized and published in Koštál et al. (2016). The protocol used previously for cryopreservation of larvae of *Chymomyza costata* (*C.c.*, pale blue line, Koštál et al., 2011) was further optimized in this study (Table S1) and the optimum parameters (ensuring the highest survival of adults) are listed in the blue frame and shown graphically as dark blue line (the rates of cooling/heating are shown as r_1, r_2, r_3 and r_4. At temperature T_1, frozen larvae are plunged into liquid nitrogen (LN$_2$), and, later, returned to Huber Ministat pre-set to T_2 temperature).

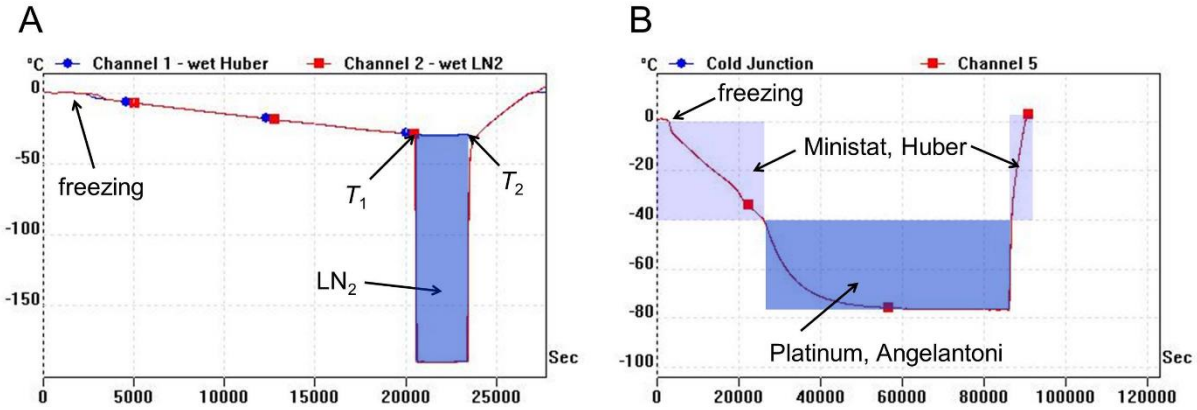

Fig. S3. Examples of temperature record from PicoLog TC-08 datalogger.

(A) Freezing to -30°C / 1h (Channel 1, blue line) and freezing to a T_1 = -30°C followed by 1h in liquid nitrogen (LN$_2$, Channel 2, red line). Note that both channels show freeze exotherms (water in the cellulose wrapping) extending over approximately 1st hour of slow cooling (rate 0.1°C min^{-1}). External ice crystals inoculate larvae inside the wrapping (see Fig. S1 E). (B) Slow freezing to -40°C in Ministat (Huber) followed by transfer to Platinum freezer (Angelantoni), where the sample gradually cooled to -75°C (Channel 5, red line).

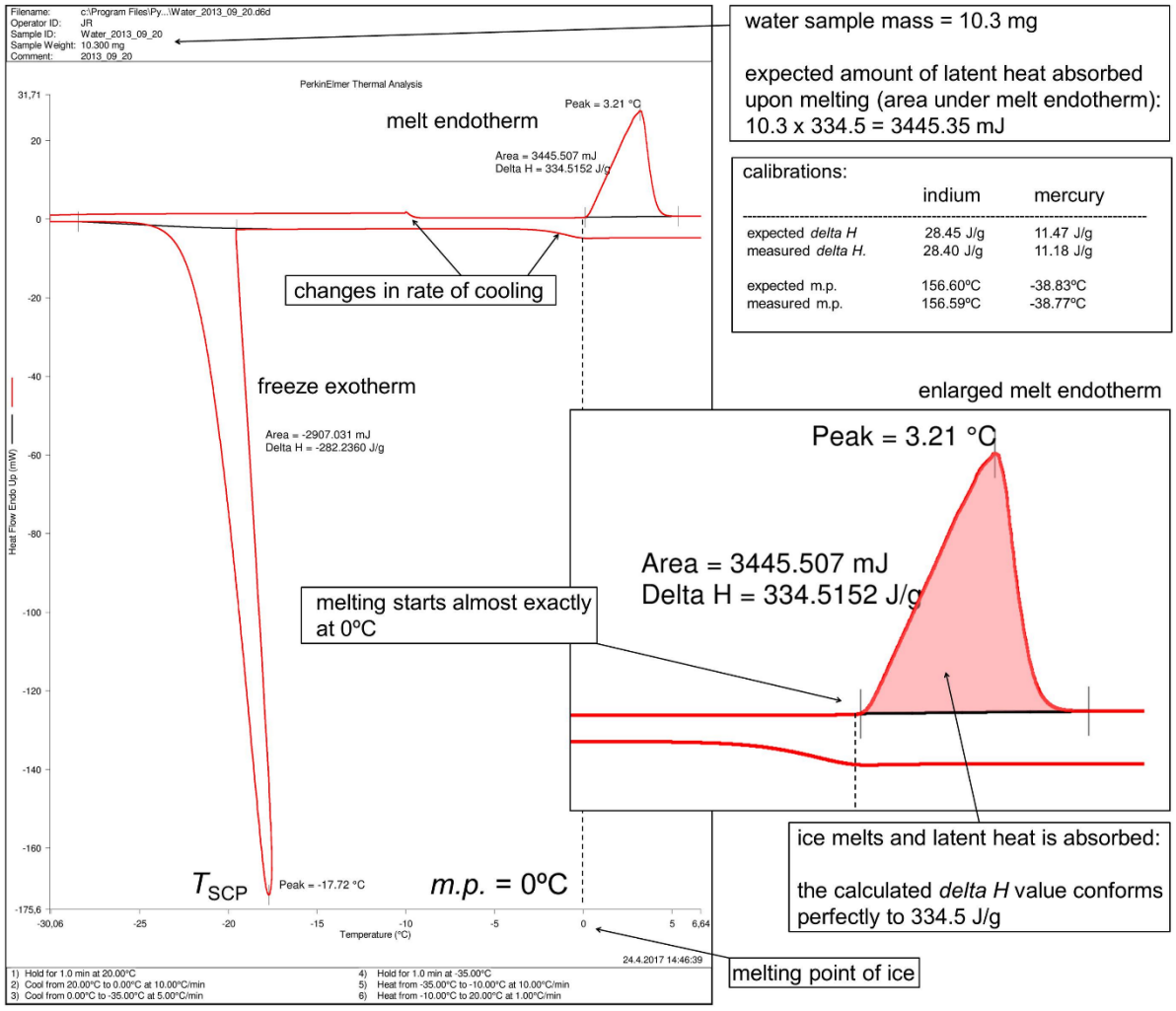

Fig. S4. DSC calibration: example protocol (distilled water).

The temperature scale and the heat flow of DSC4000 instrument were calibrated using indium, mercury and distilled water standards. Calibration parameters for indium and mercury are shown in the frame (right). An example protocol (left) shows that running the thermal analysis of distilled water sample (10.3 mg) returns expected values of melting point (m.p., 0ºC) and specific enthalpy of ice/water transition (*delta H*, 334.5 J g^{-1}) (Wang and Weller, 2011).

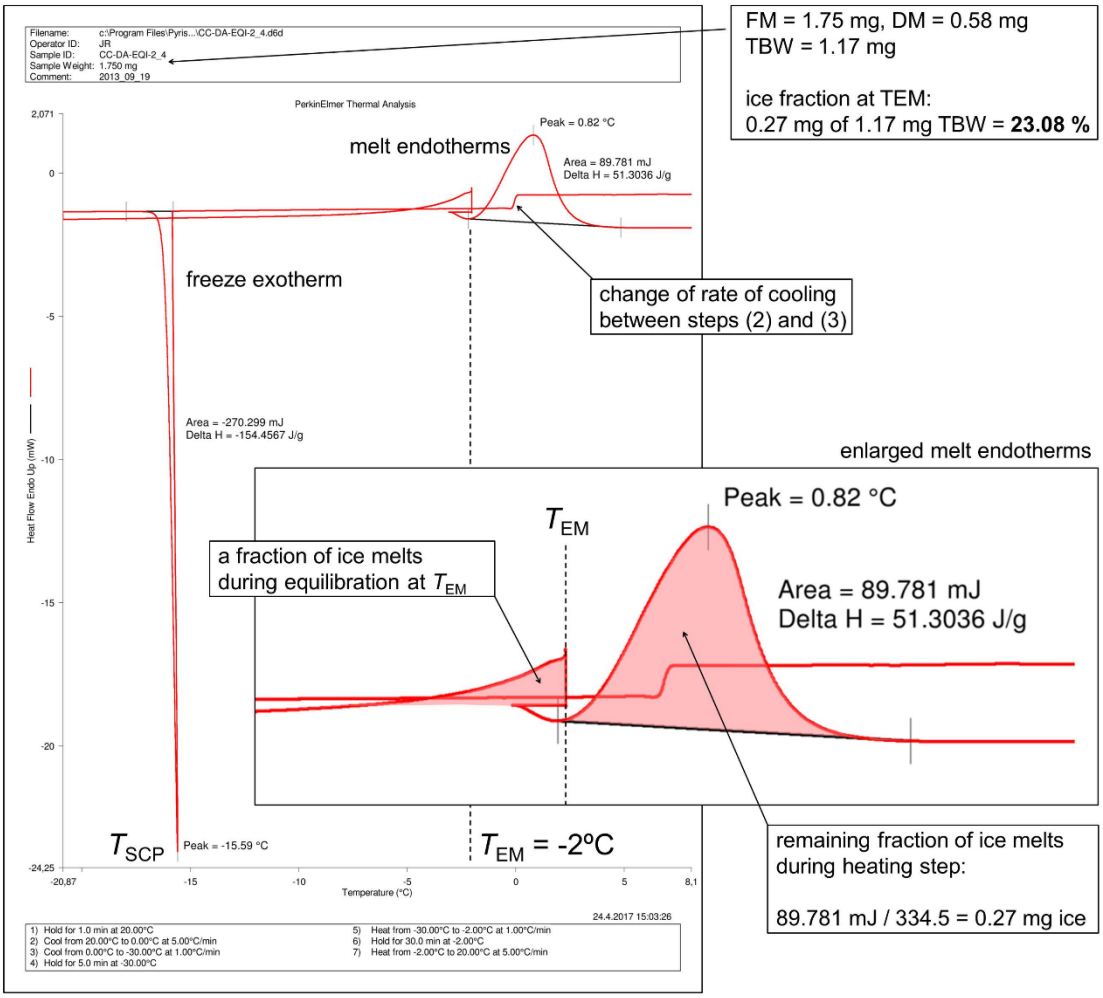

Fig. S5. *Equi-melt* thermal analysis: example protocol (*C. costata*, SDA).

The *Equi-melt* temperature programme: (1) hold for 1 min at 20ºC; (2) cool to 0ºC at a rate 5ºC min^{-1}; (3) cool to -30ºC at a rate 1ºC min^{-1}; (4) hold for 5 min at -30ºC; (5) heat to *Equi-melt* temperature (T_{EM}) at a rate 1ºC min^{-1}; (6) hold for 30 min at T_{EM}; (7) heat to 20ºC at a rate 5ºC min^{-1}.

Notes:

steps (3 and 4): the temperature of -30ºC was sufficient to reach maximum ice fraction in all treatments. We verified in preliminary experiments that neither exposing the larvae to lower temperature (down to -70ºC), nor extending the time of exposure at -30ºC (up to 48 hours) did further increase the ice fraction;

steps (5 and 6): the ice fraction equilibrates to specific T_{EM} that varied from -30ºC to -0.5ºC (in addition, T_{EM} of -50ºC was analyzed for *C. costata* SDA variant, see Fig. S7 C);

step (7): the ice fraction was calculated from the area under melt endotherm using the value of *delta H* = 334.5 J g^{-1} as the enthalpy of ice/water transition.

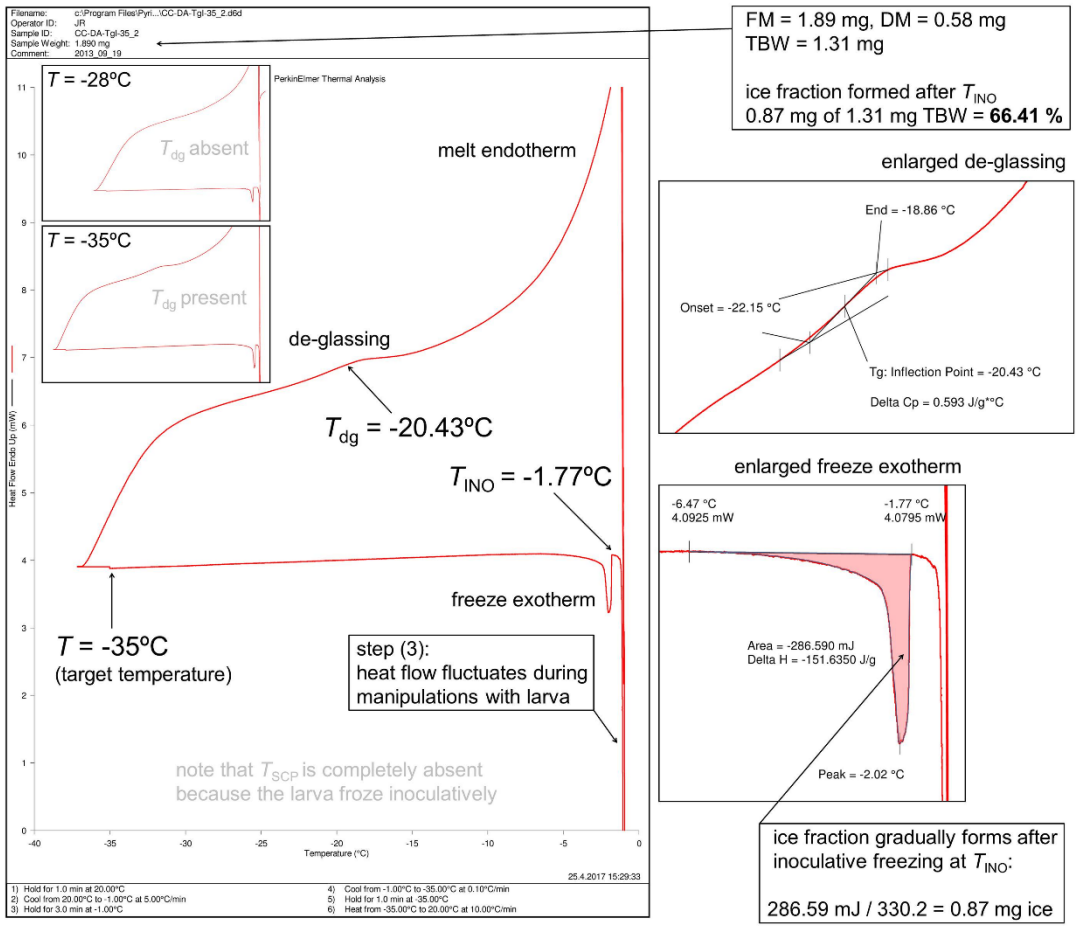

Fig. S6. *Ino-freeze* thermal analysis: example protocol (*C. costata*, SDA).

The *Ino-freeze* temperature programme: (1) hold for 1 min at 20°C; (2) cool to -1°C at a rate 5°C min^{-1}; (3) hold for 3 min -1°C and, meanwhile, open the instrument and insert aluminum pan bottom lined with filter paper disc (SS-033, Wescor) to which 10 uL of distilled water was applied and then submerged in liquid nitrogen to freeze it. Next, after the bottom of test-pan equilibrates to programmed temperature of -1°C (approximately within 10 sec), add larva, cover the bottom loosely with lid and close the instrument; (4) cool to target temperature at a rate 0.1°C min^{-1}; (5) hold for 1 min at target temperature; (6) heat to 20°C at a fast rate 10°C min^{-1}.

Notes:

steps (1 and 2): performed with the reference pan only inside instrument;

step (3): the test pan and larva were added. When performed carefully, this critical step ensures that all larvae are exposed to external ice crystals at exactly -1°C;

steps (4 and 5): the target temperature can be varied in order to see whether or not the de-glassing transition (T_{dg}) occurs upon rapid heating back to 20°C [when it occurs, it indicates that the vitrification transition (T_g) must have occurred during previous slow cooling to target temperature. Otherwise, glass trasition is not observable by DSC method at slow cooling rates]. However, observing only the specific aim of inoculative ice fraction analysis, the target temperature of -10°C would be sufficient as all larval freeze exotherms ended between -3°C and -5°C (see data in Fig. S11). The ice fraction was calculated from freeze exotherms and the enthalpy of water/ice transition (*delta H*) was modified according to the exact peak temperature of inoculative freezing (T_{INO} = -2.02°C in this example) using the formula:

$delta\ H = 334.5 + 2.12\ T_{INO} + 0.0042\ (T_{INO})^2 = 330.2$ (Wang and Weller, 2011)

step (6): the fast rate of heating (10°C min^{-1}) facilitates the observation of de-glassing (T_{dg}) transition.

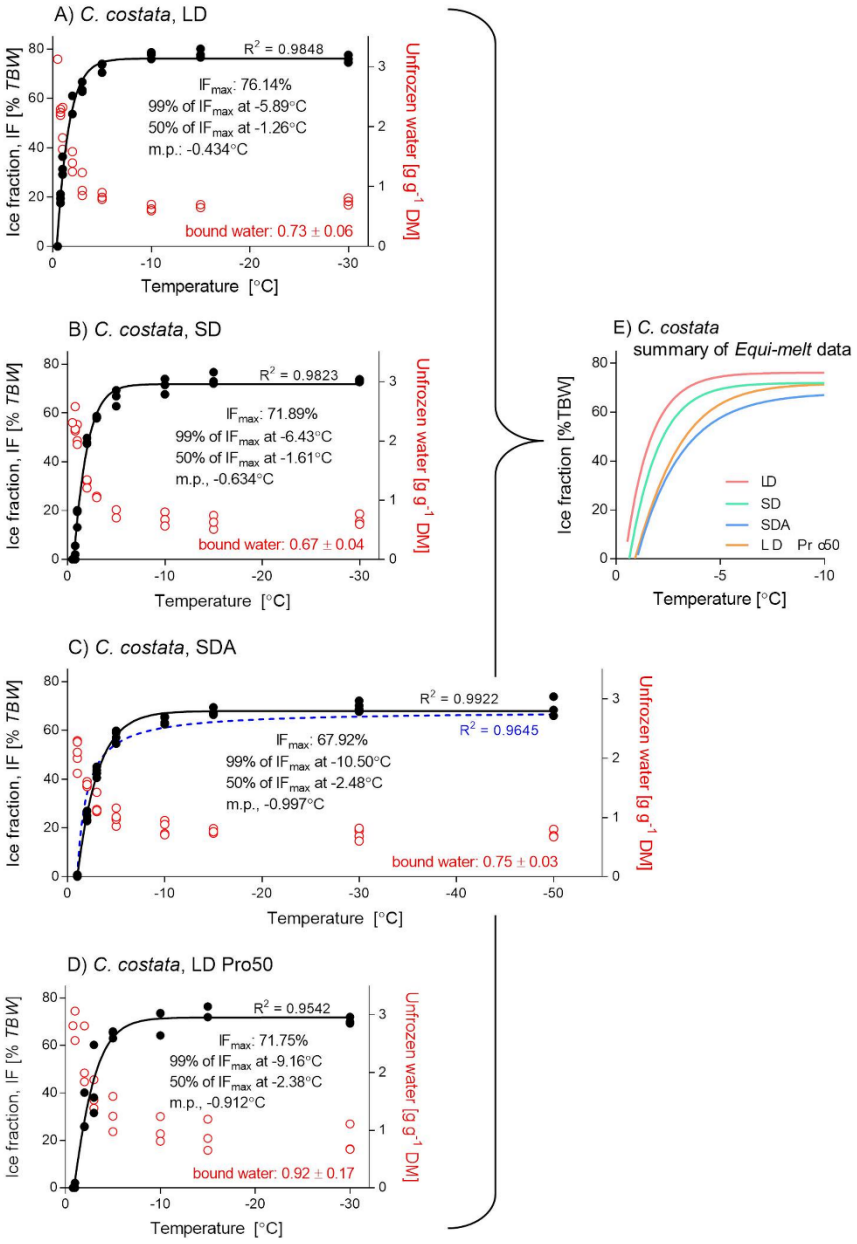

Fig. S7. Summary of *Equi-melt* data for *Chymomyza costata*

The *Equi-melt* thermal analyses were run with different target temperatures (*T*) ranging between -0.5°C and -30°C (or -50°C in SDA variant). At least three larvae were analyzed for each experimental variant (A-D) and target temperature combination (three data-points). The Boltzmann sigmoids were fitted to empirical data (black solid lines). For comparison, an example of a theoretical freezing curve (dashed blue line) *vs.* Boltzmann sigmoid fitting is shown in (C):

theoretical freezing curve (Wang and Weller., 2011): $IF = OAW*(1 - (m.p./T)$

Boltzmann sigmoid: $IF = OAW + (top – OAW)/(1 + \exp((V50-x)/slope))$

All other parameters (IF_{max}; 99% of IF_{max}; 50% of IF_{max}; m.p.) were derived from Boltzmann sigmoids. The amount of unfrozen water per mg DM for each larva is shown as red circle. Bound water (OIW) is calculated as a bottom of a Boltzmann sigmoid fitted to unfrozen water data.

(E) A summary figure showing only the *Equi-melt* curves for each treatment (these lines are used in Fig. 2A).

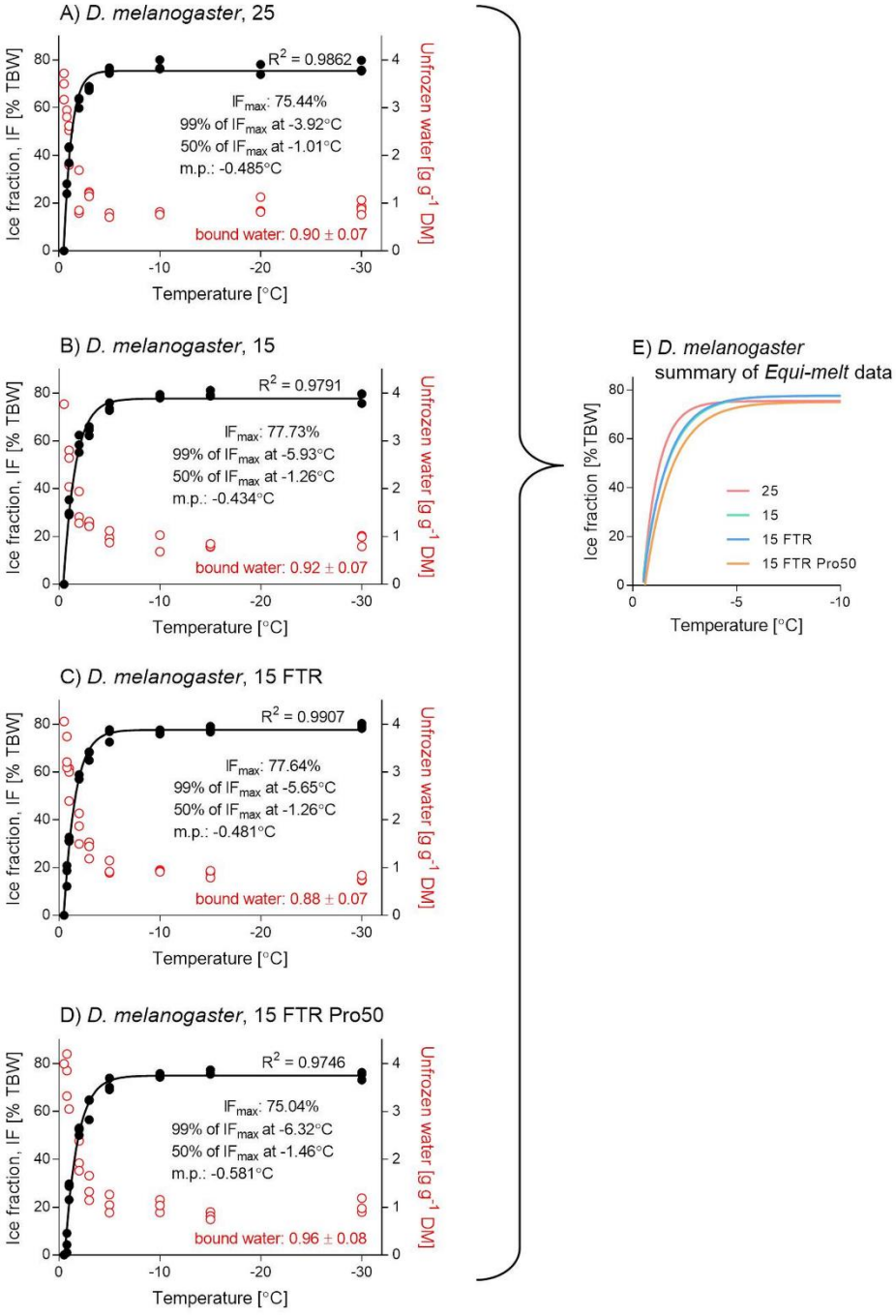

Fig. S8. Summary of *Equi-melt* data for *Drosophila melanogaster*.

All descriptions as in Fig. S7**.**
(E) A summary figure showing only the *Equi-melt* curves for each treatment (these lines are used in Fig. 2E).

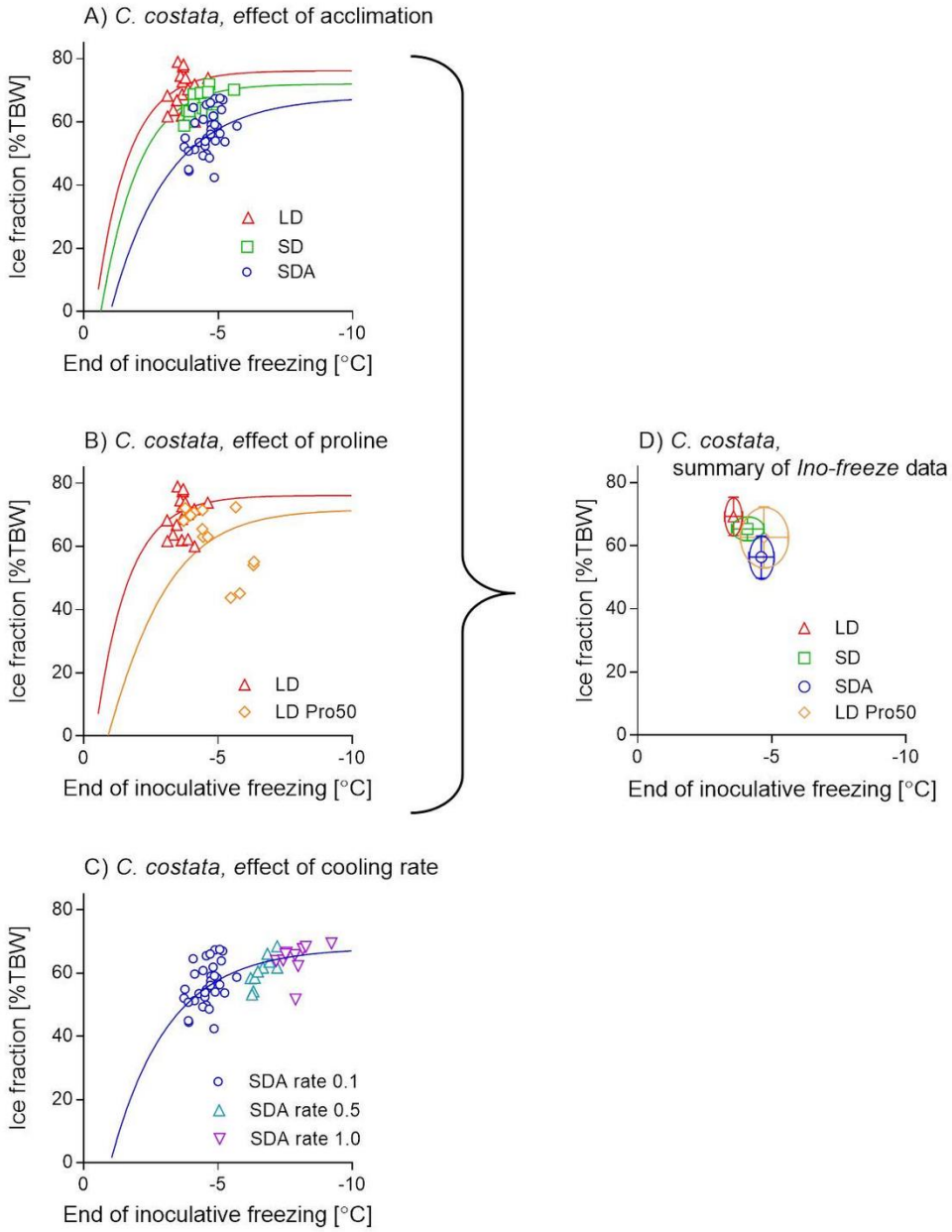

Fig. S9. Summary of *Ino-freeze* data for *Chymomyza costata*.

The *Ino-freeze* thermal analyses were run for individual larvae (points). Detailed results of *Ino-freeze* analyses are summarised in Fig. S11. *Equi-melt* curves (taken from Fig. S7) are also shown in order to allow direct comparison of the ice fraction analyzed by two methods. Note that *Ino-freeze* points and *Equi-melt* lines match very well. (A) Three acclimation variants (treatments LD, SD, SDA). (B) The effect of proline augmented diet (LD *vs.* LD Pro50). (C) The effect of cooling rate during the step (ii.) of freezing protocol. Three different cooling rates were compared: 0.1°C min^{-1}; 0.5°C min^{-1}; 1°C min^{-1}. The points express the ice fraction calculated from area under inoculative freeze exotherm at a temperature corresponding to the end of inoculative freezing (see Fig. S6).
(D) A summary figure showing ellipses based on mean x ± S.D. and mean y ± S.D. values of all *Ino-freeze* data points for each treatment (these ellipses are used in Fig. 2A).

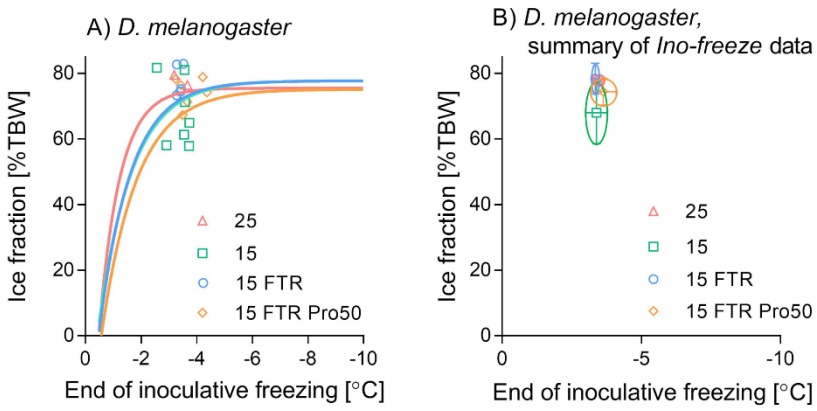

Fig. S10. Summary all *Ino-freeze* data for *Drosophila melanogaster*

All descriptions as in Fig. S9**.**
(B) A summary figure showing ellipses based on mean x ± S.D. and mean y ± S.D. values of all *Ino-freeze* data points for each treatment (these ellipses are used in Fig. 2E).

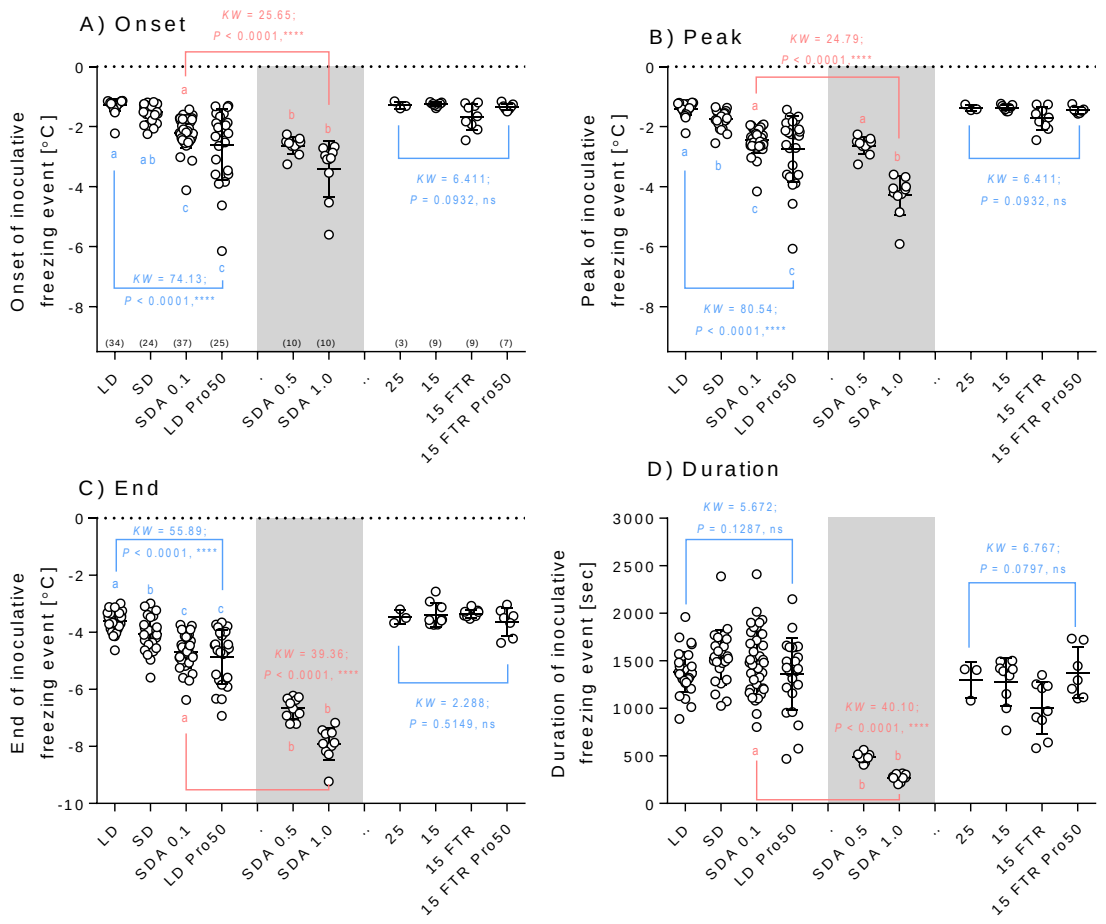

Figure S11. Summary of data obtained by *Ino-freeze* thermal analyses.

The parameters of inoculative freezing event [onset (= T_{INO}), peak, end, and duration; see Fig. S6 for more explanations] in variously treated larvae of *C. costata* (LD, SD, SDA, LD Pro50) and *D. melanogaster* (25, 15, 15 FTR, 15 FTR Pro50). In addition, the effect of cooling rate during the step (ii.) of freezing protocol was analyzed in *C. costata*. Three different cooling rates were compared: 0.1°C min^{-1}; 0.5°C min^{-1}; 1°C min^{-1}. Each point represents single thermal analysis (single larva). Number of larvae analyzed in each treatment (n) is shown in parentheses in (A). Note that there is a good match between the data on onset of inoculative freezing analyzed by DSC (Fig. S11 A) and similar data recorded directly by thermocouples in freeze-tolerance assays (Fig. S1 F). The differences between treatments (shown by blue and red lines) were assessed using Kruskal-Wallis nonparametric test (*KW* statistics is shown) followed by Dunn's multiple comparison test. Treatments flanked by different letter were statistically different according to the Dunn's test.

References

Block, W., Bauer, R. (2000). DSC studies of freezing in terrestrial enchytraeids (Annelida: Oligochaeta). *CryoLett*. **21**, 99-106.

Block, W., Wharton, D.A. andSinclair, B.J. (1998). Cold tolerance of a New Zealand alpine cockroach, *Celatoblatta quinquemaculata*. *Physiol. Entomol.* **23**, 1-6.

Gehrken, U., Southon, T.E. (1997). Effect of temperature on cold-hardiness and tissue ice formation in the adult chrysomelid beetle Melasoma collaris L. *J. Insect Physiol.* **43**, 587-593.

Halberg, K.A., Persson, D., Ramlov, H., Westh, P., Kristensen, R.M. and Mobjerg, N. (2009). Cyclomorphosis in Tardigrada: adaptation to environmental constraints. *J. Exp. Biol.* **212**, 2803-2811.

Hengherr, S., Worland, M.R., Reuner, A., Brümmer, F. and Schill, R.O. (2009). Freeze tolerance, supercooling points and ice fromation: comparative studies on the subzero temperature survival og limno-terrestrial tardigrades. *J. Exp. Biol.* **212**, 802-807.

Koštál, V., Zahradníčková, H. and Šimek, P. (2011). Hyperprolinemic larvae of the drosophilid fly, *Chymomyza costata*, survive cryopreservation in liquid nitrogen. *Proc. Natl. Acad. Sci. USA* **108**, 13035-13040.

Koštál, V., Korbelová, J., Štětina, T., Poupardin, R., Colinet, H., Zahradníčková, H., Opekarová, I., Moos, M. and Šimek, P. (2016). Physiological basis for low-temperature survival and storage of quiescent larvae of the fruit fly *Drosophila melanogaster*. *Sci. Rep.* **6**, 32346.

Lee Jr., R. E., Lewis E. A. (1985), Effect of temperature and duration of exposure on tissue ice formation in the gall fly *Eurosta solidaginis* (Diptera, Tephritidae). *Cryo-Lett*. **6**, 25-34.

Patricio Silva, A.L., Holmstrup, M., Kostal, V. and Amorim, M.J.B. (2013). Soil salinity increases survival of freezing in the enchytraeid *Enchytraeus albidus*. *J. Exp. Biol.* 213, 2732-2740.

Ramlov, H., Westh, P. (1993). Ice formation in the freeze-tolerant Alpine weta *Hemideina maori* Hutton (Orthoptera, Stenopelmatidae). *Cryo-Lett*. **14**, 169-176.

Wang, L., Weller, C.L. (2011) Thermophysical properties of frozen foods. In *Handbook of Frozen Food Processing and Packaging*, 2nd edition (ed. D.-W. Sun), pp. 101-125. Boca Raton: CRC Press.

Wharton, D. A., Block, W. (1997). Differential scanning calorimetry studies on an Antarctic nematode (*Panagrolaimus davidi*) which survives intracellular freezing. *Cryobiol.* **34**, 114–121.

Worland, M.R., Block, W. and Grubor-Lajsic, G. (2000). Survival of *Heleomyza borealis* (Diptera, Heleomyzidae) larvae down to -60°C. *Physiol. Entomol.* **25**, 1-5.

Zachariassen, K.E., Hammel, H.T. and Schmidek, W. (1979). Osmotically inactive water in relation to tolerance to freezing *in Eleodes blanchardi* beetles. *Comp. Biochem. Physiol. A* **63**, 203-206.